THE JOURNAL OF BIOLOGICAL CHEMISTRY VOL. 291, NO. 5, pp. 2087–2106, January 29, 2016


# Mutant B-Raf(V600E) Promotes Melanoma Paracellular Transmigration by Inducing Thrombin-mediated Endothelial Junction Breakdown*

Received for publication, October 6, 2015 Published, JBC Papers in Press, October 26, 2015, DOI 10.1074/jbc.M115.696419

**Pu Zhang[‡§1,2], Shan Feng[‡1], Gentao Liu[¶], Heyong Wang[¶], Huifeng Zhu[‡], Qiao Ren[‡], Huiyuan Bai[‡], Changliang Fu[§], and Cheng Dong[§]**

*From the [‡]Key Laboratory of Luminescence and Real Time Analytical Chemistry, Ministry of Education, College of Pharmaceutical Sciences, Southwest University, Chongqing 400715, China, the [§]Department of Bioengineering, Pennsylvania State University, University Park, Pennsylvania 16801, and the [¶]Shanghai Pulmonary Hospital, Tongji University School of Medicine, 507 Zhengmin Road, Shanghai 200433, China*

**Background:** A prothrombotic state is one of the hallmarks of advanced cancer.
**Results:** B-Raf(V600E)-dependent thrombin release from metastatic melanoma signals focal adherens junction disassembly by triggering VE-cadherin phosphorylation and ubiquitination.
**Conclusion:** Thrombin-mediated junction breakdown allows melanoma extravasation via a paracellular route.
**Significance:** Targeting B-Raf(V600E)-mediated thrombin generation and endothelial barrier dysfunction may represent a novel therapeutic strategy to limit tumor metastasis.

**Tumor invasiveness depends on the ability of tumor cells to breach endothelial barriers. In this study, we investigated the mechanism by which the adhesion of melanoma cells to endothelium regulates adherens junction integrity and modulates tumor transendothelial migration (TEM) by initiating thrombin generation. We found that the B-Raf(V600E) mutation in metastatic melanoma cells up-regulated tissue factor (TF) expression on cell membranes and promoted thrombin production. Co-culture of endothelial monolayers with metastatic melanoma cells mediated the opening of inter-endothelial spaces near melanoma cell contact sites in the presence of platelet-free plasma (PFP). By using small interfering RNA (siRNA), we demonstrated that B-Raf(V600E) and TF silencing attenuated the focal disassembly of adherens junction induced by tumor contact. Vascular endothelial-cadherin (VE-cadherin) disassembly was dependent on phosphorylation of p120-catenin on Ser-879 and VE-cadherin on Tyr-658, Tyr-685, and Tyr-731, which can be prevented by treatment with the thrombin inhibitor, hirudin, or by silencing the thrombin receptor, protease-activated receptor-1, in endothelial cells. We also provided strong evidence that tumor-derived thrombin enhanced melanoma TEM by inducing ubiquitination-coupled VE-cadherin internalization, focal adhesion formation, and actin assembly in endothelium. Confocal microscopic analysis of tumor TEM revealed that junctions transiently opened and resealed as tumor cells accomplished TEM. In addition, in the presence of PFP, tumor cells preferentially transmigrated via paracellular routes. PFP supported melanoma transmigration under shear conditions via a B-Raf(V600E)-thrombin-dependent mechanism. We concluded that the activation of thrombin generation by cancer cells in plasma is an important process regulating melanoma extravasation by disrupting endothelial junction integrity.**

Melanoma is the most invasive and metastatic form of skin cancer. Melanoma metastasis is a highly coordinated process, involving surviving blood's mechanical shear force, tethering onto endothelium, developing shear-resistant adhesion, disrupting endothelial barrier function, and invading underlying tissues (1, 2). Metastasis is accompanied by secretion of soluble factors, including proteases and cytokines into the extracellular milieu, which performs autocrine or paracrine roles to further promote metastasis. Hematogenous dissemination of melanoma is clearly linked with thrombosis and activation of blood coagulation. Cancer patients often have abnormal blood coagulation with elevated levels of fibrinopeptide A (3). The initiation of blood coagulation is catalyzed by the tissue factor (TF)[3]-VIIa pathway (4, 5). The transmembrane protein TF is a single-chain 263-amino acid membrane glycoprotein, which binds and allosterically activates factor VII. The TF·VIIa com-

* This work was supported by Fundamental Research Funds for the Central Universities XDJK2014C176 (to P. Z.), Start-up Foundation of Southwest University Grant SWU114017 (to P. Z.), National Natural Science Foundation of China Grants NSFC-81402393 and NSFC-81572678 (to P. Z.) and in part by National Institutes of Health Grant CA-125707 (to C. D) and National Science Foundation Grant CBET-0729091 (to C. D). The authors declare that they have no conflicts of interest with the contents of this article. The content is solely the responsibility of the authors and does not necessarily represent the official views of the National Institutes of Health.
[1] Both authors contributed equally to this work.
[2] To whom correspondence should be addressed: College of Pharmaceutical Sciences, Southwest University, Beibei, Chongqing 400715, China. Tel.: 86-18621904731; Fax: 86-23-68251225; E-mail: pxz122@swu.edu.cn.

[3] The abbreviations used are: TF, tissue factor; AJ, adherens junction; VE-cadherin, vascular endothelial-cadherin; PFP, platelet-free plasma; PAR-1, protease-activated receptor-1; TC, tumor cell; HUVEC, human umbilical vascular endothelial cell; siRNA, small interfering RNA; KSR1, kinase suppressor of ras-1; VLA-4, very late antigen-4; VCAM-1, vascular cell adhesion molecule-1; LFA-1, leukocyte function associated antigen-1; ICAM-1, intercellular cell adhesion molecule-1; ERK, extracellular signal-regulated kinases; ARMS, amplification refractory mutation system; TEM, transendothelial migration; TER, transendothelial electrical resistance; VEGF, vascular endothelial growth factor; Fo, forward; Ro, reverse; Fiwt, forward wild-type identifying; Rimut, 5 reverse mutation identifying.

plex cleaves factor IX and X, leading to the generation of serine protease thrombin. TF is highly expressed on metastatic melanoma cell lines (6). In addition, tumor dissemination is associated with TF expression. Studies with the highly specific thrombin inhibitor hirudin have revealed that thrombin in the tumor microenvironment contributes to tumor metastasis and that hirudin treatment markedly suppresses spontaneous tumor metastasis *in vivo*, prolonging mouse survival (7).

B-Raf mutations have been identified in about 60–80% of human melanomas, as well as in benign nevus specimens (8–11). A thymine to adenine transversion in exon 15, leading to a V600E substitution in the BRAF kinase domain, occurs in ~60% of melanomas (9, 10). BRAF is a component of the RAS-RAF-MEK-ERK signaling pathway that plays a critical role in cell proliferation, differentiation, and survival (12). B-Raf(V600E) may play critical roles in mediating constitutive activation of downstream kinases and gene transcription, which facilitate melanoma adhesion, migration, and proliferation (13, 14). Targeted silencing of B-Raf(V600E) down-regulated the activity of MAPK, intercellular adhesion molecule-1 (ICAM-1), and IL-8, while attenuating leukocyte-mediated melanoma extravasation and the development of lung metastases (15, 16).

Thrombin is a serine protease responsible for many homeostatic functions, including conversion of soluble fibrinogen into fibrin and activation of various intercellular signaling events in circulating blood cells via protease-activated receptor-1 (PAR-1) (17). Under certain circumstances, thrombin exposure may result in cellular inflammatory responses, such as altered ICAM-1 expression on vascular endothelial cells and activation of polymorphonuclear neutrophils, which help regulate hemostasis. By inducing VE-cadherin dimer dissociation, thrombin has been implicated in endothelial junction breakdown (17). As such, thrombin exposure induces VE-cadherin cytoplasmic phosphorylation, which displaces p120-catenin and β-catenin from adherens junctions (AJ), thereby increasing endothelial permeability (18–21). VE-cadherin can be phosphorylated at a variety of tyrosine residues (20, 21). Tyrosine sites 658, 685, and 731 of VE-cadherin may be phosphorylated in response to thrombin stimulation (19). AJ breakdown and endothelial barrier function loss play essential roles in regulating tumor metastasis. Tumor cell adhesion initiates a series of signaling cascades leading to the loss of endothelial junction integrity (22, 23). However, it is unknown whether B-Raf(V600E) overexpression in malignant melanoma cells can mediate endothelial junction breakdown by catalyzing thrombin production.

In this study, we sought to link B-Raf(V600E) activity in melanoma cells with TF overexpression and thrombin generation. In addition, the effects of knockdown and ectopic expression of B-Raf(V600E) on melanoma contact-induced endothelial junction disassembly, permeability increase, and reduction of VE-cadherin-mediated cell-cell adhesion were evaluated in the presence of platelet-free plasma (PFP). The phosphorylation of VE-cadherin and p120 was assessed in response to melanoma adhesion in PFP. The roles of tumor-derived thrombin and VE-cadherin junction breakdown in regulating the routes of melanoma transendothelial migration (TEM) were investigated.

## Experimental Procedures

*Reagents*—Hirudin was from Sigma. Anti-VE-cadherin, anti-p120-catenin, and anti-β-tubulin were purchased from Cell Signaling Technology. Alexa Fluor 488 $F(ab')_2$ goat anti-mouse IgG was from Invitrogen. TransIT 2020 was purchased from Mirus Bio LLC (Madison, WI). Super Signal West Pico chemiluminescence reagent and goat anti-mouse IgG horseradish peroxidase were obtained from Thermo Scientific (Rockford, IL). S879A-p120 cDNA was kindly provided by A. Reynolds (Vanderbilt University, Nashville, TN). It was fused to GFP to monitor transfection. Anti-Tyr(P)-658 VE-cadherin and anti-Tyr(P)-731 VE-cadherin antibodies were from Chemicon (Temecula, CA). Anti-Tyr(P)-685 VE-cadherin, anti-Rab5, anti-B-Raf, anti-TF, and anti-phosphoserine antibodies were purchased from Abcam (Eugene, OR). Human TF antibody (polyclonal rabbit anti-human TF 4502) was obtained from American Diagnostica (Stamford, CT). Rabbit anti-Lys-63-linked polyubiquitin clone Apu3 and anti-ubiquitin FK2 clone antibodies were obtained from Millipore. Anti-B-Raf(V600E) (VE1) mouse monoclonal antibody was purchased from Ventana Medical Systems (Tucson, AZ). A nonspecific antibody (rabbit IgG fraction) to act as a control was from Dako (Denmark).

Cell culture HUVECs were obtained from the American Type Culture Collection (ATCC 1730-CRL) (Manassas, VA) and maintained in F-12K medium with 10% FBS, 30 μg/ml endothelial cell growth supplement, 50 μg/ml heparin (Mallinckrodt Baker), and 100 units/ml penicillin/streptomycin (Biofluids) (passages 5–8). A375M, UACC903, and Lu1205 melanoma cell lines (obtained from ATCC) were maintained in Dulbecco's modified Eagle's medium (DMEM; Gibco) supplemented with 10% FBS and 100 units/ml penicillin/streptomycin. WM35 melanoma cells (provided by Dr. Meenhard Herlyn, Wistar Institute, Philadelphia, PA) were maintained in Roswell Memorial Park Institute (RPMI) 1640 medium supplemented with 10% FBS and 100 units/ml penicillin/streptomycin. All cells were cultured in a humidified incubator at 37 °C in 5% $CO_2$.

*Amplification Refractory Mutation System (ARMS)-PCR*—The ARMS-PCR primers were as follows: forward (Fo) 5′-CTCTTCATAATGCTTGCTCTGATAG-3′ and reverse (Ro) 5′-GCCTCAATTCTTACCATCCAC-3′; forward wild-type identifying (Fiwt) 5′-GTGATTTTGGTCTAGCTACAGT-3′ and reverse mutation identifying (Rimut) 5′-CCCACTCCATCGAGATTTCT-3′. PCR was performed in a 20-μl reaction volume containing 1× buffer, 2 mM $MgCl_2$, 1 unit of HotStar *Taq*DNA polymerase (Qiagen Science, Valencia, CA), 200 μM each dNTP, 400 nM primer Fo, 200 nM primer Ro and Fiwt, 800 nM primer Rimut, and 30 ng of genomic DNA template. PCR amplification was carried out by denaturation at 95 °C for 5 min, followed by 40 cycles at 95 °C for 20 s, 68 °C for 20 s, and 72 °C for 20 s with a final extension at 72 °C for 5 min. PCR products were analyzed by 2% agarose gel electrophoresis.

*PFP Preparation*—Following the Pennsylvania State University Institutional Review Board-approved protocols (number 19311), fresh human blood was collected from healthy adults by venipuncture into a BD Vacutainer (BD Biosciences) with

sodium citrate as the anti-coagulant. To block the contact activation pathway, corn trypsin inhibitor (0.1 mg/ml final) was added. The platelet-poor plasma was prepared by centrifugation at 2500 × *g* for 15 min and then filtration through a 0.2-$\mu$m pore cellulose membrane. PFP was prepared from platelet-poor plasma with an additional centrifugation at 13,000 × *g* for 2 min at 4 °C. PFP was diluted 1:1 with PBS before the experiments. In some cases, 40 units/ml hirudin was added to the PFP 30 min before the co-culture experiments.

*Cell Adhesion Assay*—The adhesion of HUVECs to immobilized Fc and Fc-VE-cadherin (VEC-Fc) (R&D Systems) was tested as described previously (24, 25). Wells were coated with Fc or VEC-Fc (20 mg/ml) in PBS and blocked with 3% BSA. CellTracker Green 5-chloromethylfluorescein diacetate (Thermo Fisher)-labeled HUVECs ($5 \times 10^4$/well) were washed and incubated with immobilized proteins for the indicated time at 37 °C in the presence or absence of effectors. After washings, cell adhesion abilities were quantified as the percentage of total cells added using a fluorescent plate reader (PerkinElmer Life Sciences). To determine the effect of tumor-derived thrombin on VE-cadherin-mediated cell-cell adhesion, a HUVEC monolayer was co-cultured with $1 \times 10^6$/ml melanoma cells in the presence or absence of PFP. Thereafter, HUVECs were gently detached and plated on an Fc- or VEC-Fc-coated surface in the presence of co-cultured medium.

*Contact Co-culture*—Before the experiments, HUVECs were seeded on No. 1 coverslips and starved in F-12K medium with 2% FBS without the additional supplements mentioned above for 12 h at 37 °C in 5% $CO_2$. All experiments were carried out in F-12K medium with 2% FBS without additional supplements to ensure that signaling was not influenced by additional growth factors. Then, $1 \times 10^6$ DiI-stained or unlabeled melanoma cells were directly added to and co-cultured with HUVECs on coverslips with or without PFP for the indicated time periods. For immunofluorescence, adherent melanoma cells were fixed to the HUVEC monolayer. For immunoblotting, attached tumor cells were removed with $Ca^{2+}$- and $Mg^{2+}$-free PBS/EDTA.

*Transendothelial Electrical Resistance (TER)*—TER with respect to time was measured with a Millicell ERS-2 Voltohmmeter (Millipore, Billerica, MA). The final TER values were calculated as ohm·$cm^2$ by multiplying by the surface area of the transwell insert. The results are presented as a percentage compared with that of a normal HUVEC monolayer without any co-cultured cells.

*Fluorescence Imaging and Analysis*—Before the experiments, 25-mm coverslips were coated with fibronectin (1 $\mu$g/ml) and incubated at room temperature overnight under sterile conditions. Equal amounts of HUVECs were then grown to 95–99% confluency and in some cases transfected with PAR-1 siRNA or S879A-p120 plasmid. HUVECs were co-cultured with $1 \times 10^6$ DiI-stained or unlabeled melanoma cells in the presence or absence of PFP. The co-cultures were gently fixed with 5% formaldehyde in PBS for 30 min, permeabilized with 0.3% Triton X-100, and blocked with 5% calf serum and 2% goat serum. Subsequently, coverslips were incubated with anti-VE-cadherin, anti-Lys-63-linked polyubiquitin, or anti-paxillin for 2 h at room temperature. This was followed by staining with Alexa 555 or Alexa 488-conjugated anti-rabbit IgG. To image the actin filaments, rhodamine/phalloidin (1:40; Life Technologies, Inc.) was incubated with the cells. The cells on the coverslips were imaged using a Nikon Eclipse TE2000. For each experimental condition, six coverslips were viewed under a ×100 objective, and a series of six images were taken of randomized fields of view for each coverslip. Each image was then analyzed using ImageJ software version 1.32. To analyze the size and number of paxillin-containing focal adhesions, images were background-subtracted before thresholding, and segmentation was conducted to detect the edges of the focal adhesions. Then, the mean size (in pixels) and number of focal adhesions in each cell were calculated.

Disruption of VE-cadherin was identified by analysis of the discontinuity of green fluorescence at the VE-cadherin junctions between the HUVECs. The gap area in the disrupted VE-cadherin junctions was quantified as the ratio of the number of pixels in all the gaps to that of the entire view field. The regions where HUVECs were absent before the experiments were not included in the calculation.

*Isolation of Early Endosomes*—To analyze the ubiquitination of VE-cadherin in early endosomes, HUVECs were gently homogenized in homogenization buffer (250 mM sucrose, 3 mM imidazole (pH 7.4)), and the resulting post-nuclear supernatants were prepared. Post-nuclear supernatants were adjusted to 40% sucrose, overlaid with 35 and 25% sucrose, and filled with homogenization buffer containing 0.5 mM EDTA. The gradients were centrifuged at 108,000 × *g* for 3 h at 4 °C. Following centrifugation, the interface fractions were collected and subjected to immunoprecipitation. Rab5 served as a marker for early endosomes as detected by anti-Rab5 antibody (Cell Signaling Technology).

*Western Blotting*—After HUVEC-melanoma co-culture, adherent tumor cells were removed by washing 3–5 times with pre-warmed $Ca^{2+}$- and $Mg^{2+}$-free PBS/EDTA. HUVECs were rinsed with PBS and lysed with RIPA lysis buffer (20 mM Tris, 5 mM $MgCl_2$, 1 mM PMSF, 20 mg/ml aprotinin, 10 mg/ml leupeptin, 1 mM $Na_3VO_3$, and 20 mM $\beta$-glycerophosphate). The lysates were centrifuged at 14,000 rpm for 15 min. The protein concentrations across the samples were checked using the Bradford method. The samples were denatured by adding SDS running buffer (0.2% bromphenol blue, 4% SDS, 100 mM Tris (pH 6.8), and 20% glycerol) and $\beta$-mercaptoethanol. The samples were analyzed by SDS-PAGE on 12% gels. After the proteins were transferred to nitrocellulose membranes, phosphorylated VE-cadherin (Tyr-658), phosphorylated VE-cadherin (Tyr-685), and phosphorylated VE-cadherin (Tyr-731) were detected with corresponding primary monoclonal antibodies (1:1000 diluted in blocking buffer) followed by HRP-conjugated secondary antibodies. The labeled proteins were visualized using a chemiluminescence kit. Thereafter, membranes were stripped with stripping buffer before being re-probed with anti-VE-cadherin and anti-$\beta$-tubulin to ensure equal loadings.

*Immunoprecipitation*—Whole cell extracts were prepared by resuspending $2 \times 10^7$ cells in 500 $\mu$l of lysis buffer (10 mM Tris-HCl (pH 7.4), 150 mM NaCl, 1 mM EDTA (pH 8.0), 2 mM $Na_3VO_3$, 10 mM NaF, 10 mM $Na_4P_2O_7$, 1% Nonidet P-40, 1 mM PMSF, 2 ng/ml pepstatin A). Lysates were incubated on ice for 30 min followed by centrifugation at 16,000 × *g* for 5 min

at 4 °C. Pellets were discarded, and the supernatant was precleared with protein G-agarose (Santa Cruz Biotechnology). Precleared lysates were incubated with anti-p120 pre-absorbed with protein G-agarose overnight at 4 °C under continuous mixing. Pellets were collected after four washes with lysis buffer and mixed with 2× SDS running buffer (0.2% bromphenol blue, 4% SDS, 100 mM Tris (pH 6.8), 200 mM DTT, 20% glycerol) in a 1:1 ratio. Samples were boiled for 3 min, and 20 $\mu$l was loaded onto a 6% SDS-polyacrylamide gel. Proteins were transferred to a nitrocellulose membrane by electroblotting. Primary antibodies included anti-p120 and anti-phosphoserine. The secondary antibody was HRP-conjugated secondary antibody. The labeled proteins were visualized using a chemiluminescence kit. Thereafter, membranes were stripped with stripping buffer before being reprobed with anti-$\beta$-tubulin to ensure equal loadings.

For analyzing VE-cadherin ubiquitination in early endosomes, isolated early endosomes were incubated with anti-VE-cadherin-coupled protein G-agarose. Then, immunoprecipitated VE-cadherin was washed three times with dilution buffer (1% Triton X-100, 0.5% SDS, 10 mM Tris (pH 7.5), 150 mM NaCl) and twice with a washing buffer (200 mM NaCl, 400 mM NaOAc) before preparation for SDS-PAGE and Western blot analysis using a ubiquitin antibody (FK2 ubiquitin clone, Millipore).

*Reverse Transcription-Polymerase Chain Reaction (RT-PCR)*—Total RNA was extracted using an RNeasy kit (Qiagen) following the manufacturer's instructions. cDNA was synthesized from 2 $\mu$g of RNA using Takara Reverse Transcription Reagents (Takara Bio, Japan). PCR was performed with PCR master mix (Life Technologies, Inc.) by an initial denaturation step at 95 °C for 5 min, followed by 40 cycles at 95 °C for 45 s, 60 °C for 45 s, and 72 °C for 1 min. We used specific primers for human PAR-1 (sense, 5′-GGGTCTGAATTGTGTCGCTTCG-3′; antisense, 5′-GCTGCTGACACAGACACAGAGG-3′) and GAPDH (sense, 5′-GTCGTATTGGGCGCCTGGTCAC-3′; antisense, 5′-AGGGGCCATCCACAGTCTTCTG-3′). PCR products were resolved by 2% agarose gel electrophoresis and stained with ethidium bromide. Negative controls lacking reverse transcriptase were run in parallel to confirm that samples were not contaminated with genomic DNA.

*siRNA Targeting Mutant B-Raf, TF, and PAR*—1-siRNA (100 pmol) was introduced into $1 \times 10^6$ Lu1205, A375M, UACC903, WM35, or HUVEC via nucleofection with an Amaxa Nucleofector (Koeln, Germany). Solution R/program K-17 was used for the Lu1205, UACC903, WM35, or HUVEC cell lines, and Solution R/program A-23 was used for the A375M cells. The resultant transfection efficiency following nucleofection was 85%. Duplexed Stealth siRNA (Invitrogen) was used for these studies. The sequence for each respective siRNA is as follows: scrambled siRNA, 5′-AAUUCUCCGAACGUGUCACGUG AGA-3′; MUT B-RAF (accession number NM_004333.4), 5′-GGUCUAGCUACAGAGAAAUCUCGAU-3′; TF (accession number M16553), 5′-GCGCUUCAGGCACUACAAAtt-3′; PAR-1 (accession number M62424.1), 5′-CCCUGCUCGAAG-GCUACUAtt-3′. Following nucleofection, cells were replated, and 72 h later, protein lysates were harvested for Western blot or RT-PCR analysis.

*Plasmid Transfection*—HUVECs were stably transfected with GFP-S879A-p120 or control vector. 2.5-$\mu$g plasmids were transfected into HUVECs with 7.5 $\mu$g of Mirus TransIT 2020. After 24 h, the transfection efficiency was detected by Western blotting.

The pBABEbleo-FLAG-BRAF(V600E) was a gift from Christopher Counter (Addgene plasmid 53156). The pBABE-bleo was a gift from Hartmut Land, Jay Morgensten, and Bob Weinberg (Addgene plasmid 1766). The pBABEbleo-FLAG-BRAF was created by subcloning from pcDNA3-BRAF. Retroviral infection of WM35 was conducted following a previous protocol (26). To produce retrovirus, 293T cells were incubated with 12 ml of FuGENE 6, 3 mg of pCL-10A1, and 3 mg of the pBABE plasmid of interest. Then, WM35 cells ($1 \times 10^5$ per well in a 6-well plate) were infected with virus-containing media together with Polybrene (4 $\mu$g/ml). pBABEbleo-FLAG-BRAF(V600E), pBABE-bleo, and pBABEbleo-FLAG-BRAF transfected stable clones were selected with Zeocin. The transfection efficiency was assessed by Western blotting with either anti-FLAG or anti-B-Raf(V600E) antibody.

*Static Transmigration Assay*—Static transmigration assays were conducted in a conventional 48-well chemotactic Boyden chamber. To conduct the experiments, HUVECs were grown to confluency on fibronectin-coated polyvinylpyrrolidone-free polycarbonate filters (8-$\mu$m pore size; NeuroProbe). The wells on the bottom plate of the chamber were filled with collagen type IV (100 $\mu$g/ml in RPMI 1640 medium with 1% BSA) to act as a chemoattractant to melanoma cells (27, 28). Melanoma cells ($1 \times 10^6$/ml) were then loaded in the holes on the top plate of the migration chamber with or without PFP. After incubation at room temperature for 4 h, melanoma cells migrating through the endothelial layer were stained with Protocol Brand Hema 3 solution (Fisher) and imaged under an inverted microscope (Diaphot 330; Nikon). The number of migrated cells was analyzed with ImageJ software.

*Flow Transmigration Assay*—Tumor transmigration under flow conditions was determined using a modified 48-well chemotactic Boyden chamber consisting of top and bottom plates separated by a gasket. An inlet and an outlet allowing for connection to the flow loop were carved in the top plate. The bottom plate had 48 chemotactic wells and screwed around the perimeter to affix to the top plate. The gasket was an 11 × 5.5-cm 0.02-inch-thick piece of silicon (SFMedical, Hudson, MA). A 7 × 2-cm opening was cut in the center of the flow field. The wall shear stress ($\tau_w$) was related to the volumetric flow rate ($Q$) by the following formula: $\tau_w = 6\ \mu Q/wh^2$. Before each experiment, a monolayer of HUVECs was grown on polycarbonate filters (8-$\mu$m pore size; NeuroProbe, Gaithersburg, MD) pre-coated with fibronectin (30 $\mu$g/ml) (Sigma). The central 12 wells of the bottom plate were filled with soluble chemoattractant type IV collagen. The assembled chamber was primed with 0.1% BSA in DMEM to eliminate bubbles. Then, melanoma cells were drawn across the HUVEC monolayer with a peristaltic pump at a shear stress of 2 or 4 dynes/cm$^2$ for 4 h in a 37 °C, 5% $CO_2$ incubator. When the assay was completed, the flow chamber was removed from the flow loop and dissembled. The migrated cells were stained with Protocol Brand Hema3 solution (Fisher). Cells in 12 randomly selected fields were counted

using an inverted microscope (IX71, Olympus) with ImageJ software (National Institutes of Health). For each dataset, at least three filters were analyzed.

*Live Cell Imaging of Melanoma TEM*—GFP-fused VE-cadherin was generated by cloning mApple-VE-cadherin (Addgene) to GFP-pcDNA3 with BamHI and XbaI restriction sites. GFP-VE-cadherin was transfected to HUVEC with Mirus TransIT 2020. Melanoma cells were labeled with DiI (Molecular Probes) and then deposited on a monolayer of GFP-VE-cadherin-transfected HUVECs cultured on Matrigel-coated coverslips mounted on an Olympus Fluoview FV1000 confocal laser scanning microscope with a ×60 oil immersion objective. For TEM experiments, sequential images of VE-cadherin (green) and tumor (red) were taken for 4 h in representative fields. The confocal iris was set to generate a 0.3-$\mu$m-thick slice. Fluorescence was scanned on the *z* axis in 0.3-$\mu$m steps. The combined images were prepared by overlaying images of adherent and migrating tumors onto the image of the GFP-VE-cadherin fluorescence. Transmigrating tumor cells, which were more than 5 $\mu$m from junctions as identified by GFP-VE-cadherin fluorescence and did not disrupt the VE-cadherin staining, were considered to have taken a "transcellular route." The percentage of TEM = total transmigrated tumor cells/(total adherent + transmigrated tumor cells) × 100.

*Measurement of TF*—Transfected or untransfected melanoma cells were lysed and solubilized with 15 mM octyl $\beta$-D-glucopyranoside at 37 °C for 15 min. The samples were diluted 1:2 with diluent buffer. To measure TF levels, each 96-well plate was coated with mouse anti-human capture antibody diluted in $NaHCO_3$ (pH 8.2) at a final concentration of 2 $\mu$g/ml (R&D, Minneapolis, MN). After the plates were incubated overnight at 4 °C, each plate was blocked for 2 h at room temperature with PBS, 1% BSA. Samples and standards were added at 100 $\mu$l per well and incubated overnight at 4 °C. Wells were incubated for 2 h at room temperature in biotinylated detecting antibodies for TF. The plate was then washed six times and incubated with 10 $\mu$l of streptavidin peroxidase (1 $\mu$g/ml, Sigma) for 30 min at room temperature. 100 $\mu$l of 2,2′-azino-bis (3-ethylbenzothiazoline-6-sulfonic acid) diammonium salt (Sigma) peroxide substrate solution was then added. The plate was read using a microtiter plate reader at a wavelength of 405 nm. TF levels (ng/ml) were calculated by interpolating the standard curve.

*Measurement of Thrombin Generation in Co-culture*—Tumor cell samples were tested for their thrombogenic capacities using a CAT assay. PFP was incubated for 10 min with cell samples containing 4 $\mu$M phospholipids (Thrombinoscope) in round bottom 96-well microtiter plates. Thrombin generation was initiated by adding 30 $\mu$l of $CaCl_2$/fluorogenic substrate (benzyloxycarbonyl-Gly-Gly-Arg-7-amino-4-methylcoumarin; Bachem, Bubendorf, Switzerland) mixture. Fluorescence was read using a Fluoroskan Ascent reader (Thermo Lab Systems, Helsinki, Finland), and thrombin generation curves were calculated using Thrombinoscope software. The thrombin generation curves were considered cell line-specific when the signal was higher than that obtained with PBS only (*i.e.* no cells).

*Statistical Analysis*—Data were obtained from at least three independent experiments and are expressed as mean ± S.E. Statistical significance of differences between means was determined by using a Student's *t* test or analysis of variance. Tukey's test was used for post hoc analysis of variance. Probability values of $p < 0.05$ were deemed to be statistically significant.

## Results

*Targeting Mutant B-Raf(V600E)-TF Signaling in Melanoma Cells Inhibited Thrombin Generation*—Melanoma harboring the B-Raf(V600E) mutation has been shown to enhance adhesion-independent growth, alter $G_1$-S cell cycle progression, and exacerbate leukocyte-mediated metastasis (15, 16, 29–31). Melanoma patients who achieved metastatic disease remission after receiving a B-Raf(V600E) inhibitor, Vemurafenib, tended to have down-regulated levels of thrombin generation and D-dimer, indicating a possible association between hypercoagulation and the BRAF(V600E) mutation in metastatic melanoma (32). However, the cross-talk mechanism between melanoma, coagulation factors, and endothelium leading to melanoma metastasis remains unknown. To develop a thorough understanding of the role of B-Raf(V600E) in thrombogenesis, we analyzed the expression levels of mutant B-Raf in four melanoma cell lines, WM35 (non-metastatic), A375M (median metastatic), UACC903 (median metastatic), and Lu1205 (highly metastatic) with different metastatic potentials using ARMS-PCR (33) and Western blotting. Expression of B-Raf(V600E) in melanoma cells carrying the T1799A mutation correlated with melanoma metastatic potential. WM35 expressed the lowest and Lu1205 expressed the highest metastatic potential (Fig. 1, *A* and *B*). Membrane TF expression on the melanoma cell lines was also associated with the malignancy and invasiveness of melanoma (WM35, 10.5 ± 1.2 ng/ml; Lu1205,145.0 ± 7.6 ng/ml) (Fig. 1*B*). Therefore, we postulated that the B-Raf mutation initiates downstream signaling leading to TF overexpression and TF-based thrombogenesis. siRNA was specifically designed and nucleofected to suppress the expression of mutant B-Raf(V600E) in melanoma cell lines. Nucleofection resulted in siRNA knockdown efficiencies of 85% (Fig. 1*C*). Knockdown of B-Raf(V600E) protein in A375M, UACC903M, and Lu1205 cells persisted for 6 days in culture compared with control cells nucleofected with scrambled siRNA (data not shown). Knockdown of B-Raf(V600E) significantly down-regulated TF protein levels on Lu1205, UACC903, and A375M cells compared with scrambled siRNA and buffer controls ($p < 0.05$) (Fig. 1*C*). To determine whether mutant B-Raf drives thrombin generation, the dynamic thrombin generation was measured with Lu1205 cells in PFP that was depleted of platelets but retained all pro-coagulant factors, including factors Xa and Va. Compared with buffer or scrambled siRNA-transfected cells, B-Raf(V600E)-silenced Lu1205 cells had a markedly lower thrombin generation potential with longer lag time and lower peak thrombin levels as measured by CAT (Fig. 1*D*). To verify that TF is located downstream of B-Raf(V600E) to trigger thrombin production, TF was silenced with siRNA before the measurement of thrombin generation. >85% siRNA knockdown efficiency of TF was achieved in

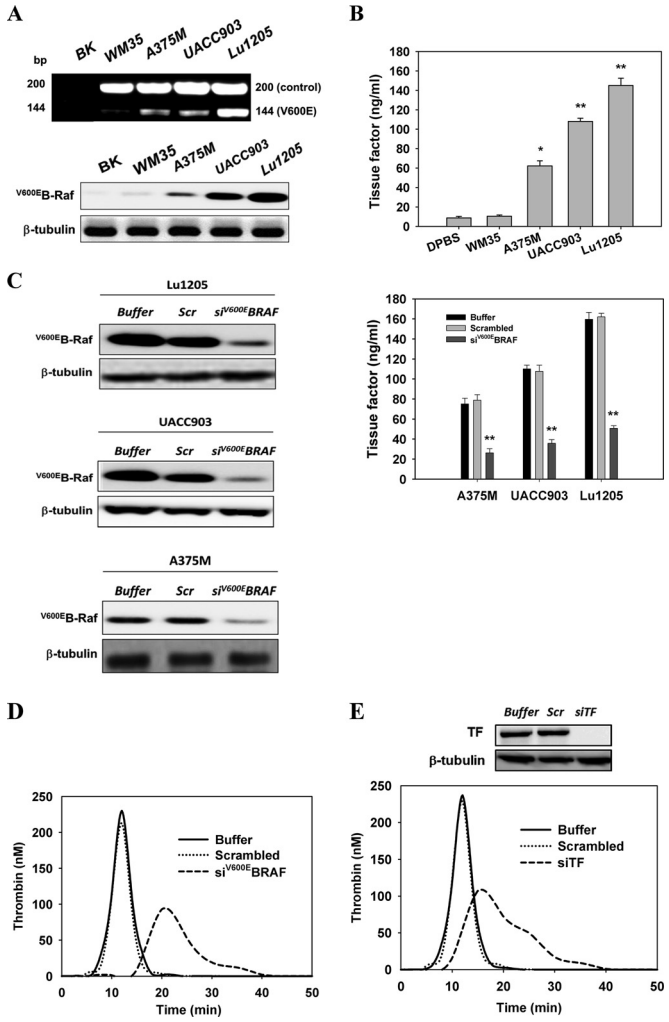


FIGURE 1. **B-Raf(V600E) mutation conferred on melanoma a thrombogenic potential by inducing TF expression.** *A,* ARMS-PCR and Western blotting were used to detect the presence of B-Raf(V600E) in the WM35, A375M, UACC903, and Lu1205 melanoma cell lines. The Fo-Ro primer pair generated a common fragment of 200 bp flanking the mutation site. The Fo-Rimut primer pair generated the 144-bp fragment specific for the B-Raf(V600E) gene. *BK*, blank no DNA (control). Anti-B-Raf(V600E) (VE1) antibody was used to detect B-Raf(V600E) protein levels. *B,* cell membrane fractions from four melanoma cell lines were isolated with octyl β-D-glucopyranoside, and TF expression was measured by ELISA. TF levels (nanograms/ml) are shown as means of three independent experiments ± S.E. *, $p < 0.05$; **, $p < 0.01$ compared with control cases. *C,* knockdown of B-Raf(V600E) with siRNA in A375M, UACC903 and Lu1205 cells significantly reduced TF expression. A375M, UACC903, and Lu1205 cells transfected with buffer, scrambled siRNA, or B-Raf(V600E) siRNA were subjected to TF measurement. TF levels (nanograms/ml) are shown as means of three independent experiments ± S.E. **, $p < 0.01$ compared with control cases. Knockdown efficiency was assessed by Western blotting. *Scr,* scrambled; *siV600EBRAF*, B-Raf(V600E) siRNA. *D,* knockdown of B-Raf(V600E) with siRNA in Lu1205-impaired thrombin generation. Thrombin activities were measured with a calibrated automated thrombogram. *E,* knockdown of TF with siRNA in Lu1205 cells suppressed thrombin generation. Thrombin activities were measured with a calibrated automated thrombogram. Knockdown efficiency was assessed by Western blotting. *siTF*, TF siRNA.

Lu1205 cells (Fig. 1*E*). Similar levels of siRNA-mediated TF knockdown cells were observed for A375M and UACC903 cells (data not shown). TF abrogation reduced peak thrombin levels 2.2-fold and prolonged the lag time. This implies that B-Raf(V600E) promotes TF overexpression, which in turn results in enhanced thrombin generation in metastatic melanoma cells.

*AJ Dissociation Occurred in Close Proximity to Melanoma Contacts in the Presence of Plasma*—Thrombin treatment disrupts endothelial barrier function, which is accompanied by VE-cadherin dimer disassembly and internalization (17, 18, 34–36). To assess whether the thrombogenic capacities of melanoma cells are associated with their tendency to induce endothelial AJ breakdown, VE-cadherin was immunofluorescently stained to visualize endothelial gap formation upon melanoma contact when co-cultured with or without PFP. Melanoma cells were allowed to settle freely onto the HUVEC monolayer. They randomly attached to the HUVEC monolayer in the immediate vicinity of junctions (bicellular or tricellular corners) or in the apical regions of HUVECs remote from the junction sites. As shown in Fig. 2*A*, AJs remained intact by co-culturing Lu1205 or UACC903 and HUVECs in the absence of PFP for 60 min. VE-cadherin staining was most prominent around the cell periphery, suggesting that the assembly of VE-cadherin dimers was maintained at AJs. In sharp contrast, PFP treatment disrupted AJs upon Lu1205 or UACC903 contact (Fig. 2*A*). Furthermore, VE-cadherin staining was weakened at the cell periphery, implying that VE-cadherin was either translocated or internalized. Interestingly, gaps were mainly formed in close proximity to the adherent melanoma cells. AJ dissociation was not observed in the regions where tumor cells were absent. In response to the focal loss of VE-cadherin dimers, melanoma cells extended their pseudopod protrusions toward the sites of loss of VE-cadherin dimers in the junctions. In addition, separate co-culture of HUVECs and melanoma cells in the transwell systems did not result in endothelial AJ breakdown (data not shown). These findings suggest that melanoma cells need to physically contact endothelial cells to effect gap formation. However, it seemed that receptor-ligand-mediated cell-cell adhesion was not required for this process, because simultaneous knockdown of CD44 and VLA-4, the two primary receptors for melanoma adhesion to endothelium, did not alter the ability of melanoma to induce AJ dissociation in PFP (37, 38).

Quantification of the gap sizes revealed that A375M, UACC903, and Lu1205 melanoma cells, which carried high levels of B-Raf(V600E), created significantly larger gap areas through contact with HUVECs in the presence of PFP than in the absence of PFP ($p < 0.05$), whereas WM35 with low B-Raf(V600E) expression did not induce VE-cadherin junction disassembly even in the presence of PFP (Fig. 2*B*). Of note, PFP did not mediate the gap formation *per se* (no TC: −PFP *versus* +PFP) (Fig. 2*B*). To examine the possible effect of melanoma contact on the integrity of the endothelial barrier, we measured TER. In the presence of PFP, Lu1205 but not WM35 contact reduced the electrical resistance of endothelium in a time-dependent manner (Fig. 2*C*). Co-culture of Lu1205 and HUVEC in PFP resulted in a reduction of endothelial electrical resistance by 42% at 100 min.

Knockdown of B-Raf(V600E) attenuated endothelial gap formation induced by Lu1205 and UACC903 cells in the presence of PFP (Fig. 2*D*). Similarly, siRNA-based knockdown or antibody blocking of TF dramatically suppressed Lu1205/PFP-mediated endothelial junction disassembly (Fig. 2*E*). Treatment with thrombin inhibitor, hirudin, which specifically blocks

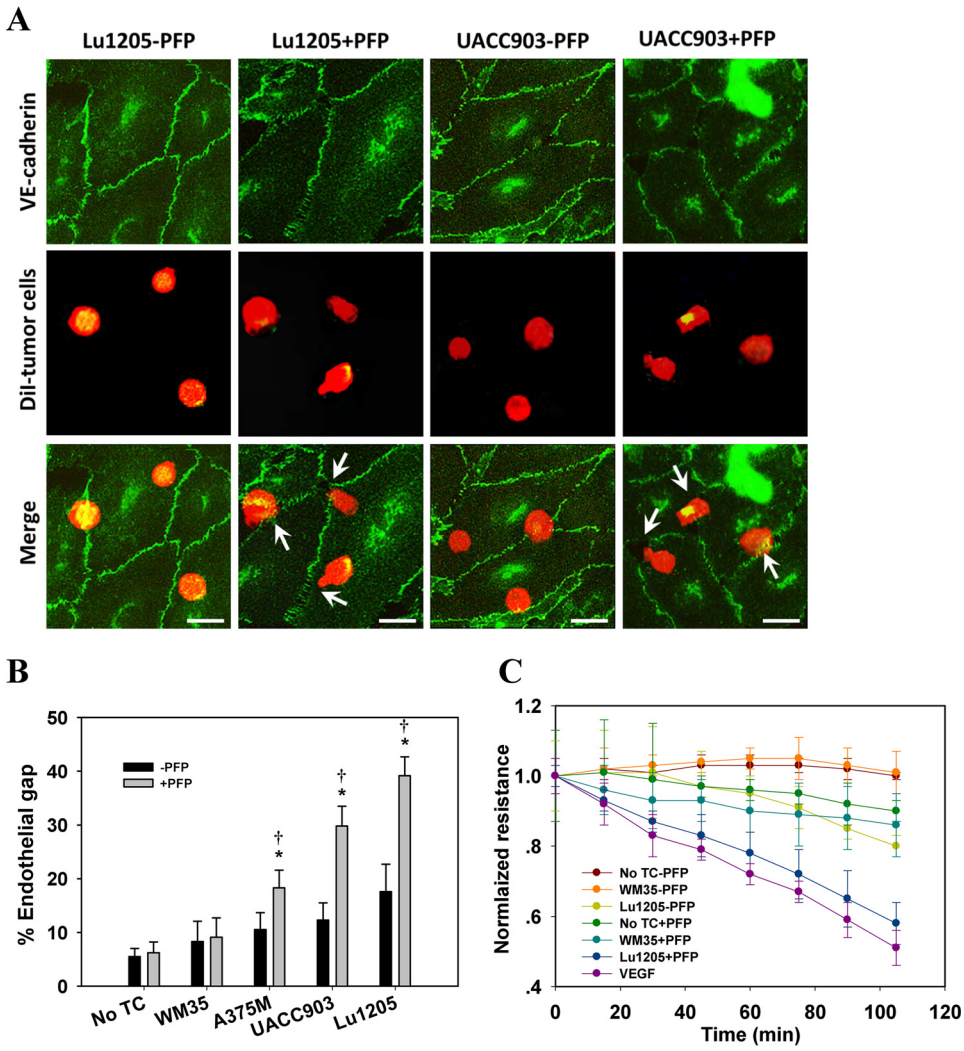


FIGURE 2. **Melanoma contacts increased endothelial gap formation and permeability in a B-Raf(V600E)- and PAR-1-dependent manner.** *A,* gaps in AJ were formed at the sites of melanoma adhesion in the presence of PFP. $1 \times 10^6$ Lu1205 or UACC903 cells that were stained with DiI were co-cultured with a HUVEC monolayer for 60 min in the presence (+*PFP*) or absence of PFP (−*PFP*) before the VE-cadherin was stained. With PFP, Lu1205 or UACC903 contacts induced gap formation and reduced VE-cadherin staining at the cell periphery. *White arrows* indicate the locations of junction dissociation and tumor pseudopod protrusion. *Bar,* 5 $\mu$m. *B,* percent endothelial gaps significantly increased upon melanoma-HUVEC co-culture in the presence of plasma. $1 \times 10^6$ WM35, A375M, UACC903, and Lu1205 melanoma cells were co-cultured with a HUVEC monolayer for 60 min in the presence or absence of PFP before the endothelial gap area was determined. *, $p < 0.05$ compared with −PFP; †, $p < 0.05$ compared with no TC control. *C,* HUVECs were grown on transwell inserts with 0.4-$\mu$m pores before being left alone or co-cultured with WM35 or Lu1205 melanoma cells with or without PFP for the indicated time periods. HUVEC monolayer TER was measured as described under "Experimental Procedures." The time-dependent change of the electrical resistance of HUVEC monolayer stimulated with 80 ng/ml VEGF served as a positive control. *D,* silencing B-Raf(V600E) with siRNA in late-stage melanoma cells, Lu1205 and UACC903, resulted in a dramatic decrease in gap formation in the presence of, but not in the absence of, PFP. *, $p < 0.05$ compared with control cases. *si$^{V600E}$BRAF*, B-Raf(V600E) siRNA. *E,* depletion of TF with siRNA or blocking of TF with antibody-attenuated Lu1205/PFP-induced gap formation. *, $p < 0.05$ compared with control cases (buffer, scrambled, or isotype control). *F,* anti-coagulant, hirudin, reduced Lu1205/PFP-induced gap formation. *, $p < 0.05$ compared with vehicle control. *G,* HUVECs were grown on transwell inserts with 0.4-$\mu$m pores before co-culturing with Lu1205 melanoma cells transfected with buffer, scrambled siRNA, B-Raf(V600E) siRNA (*si$^{V600E}$BRAF*), or siTF, or treated with vehicle control or 40 units/ml hirudin with PFP for indicated time periods. HUVEC monolayer TER was measured as described in "Experimental Procedures." The time-dependent changes in the electrical resistance of the HUVEC monolayer, which was left alone or stimulated with 80 ng/ml VEGF, served as controls. *H,* depletion of PAR-1 with siRNA attenuated Lu1205- or UACC903/PFP-induced gap formation. *, $p < 0.05$ compared with control cases (buffer or scrambled). Knockdown efficiency was assessed by PCR. *siPAR-1*, PAR-1 siRNA. *I,* HUVECs transfected with buffer, scrambled siRNA, or siPAR-1 were grown on transwell inserts with 0.4-$\mu$m pores. Then they were co-cultured with Lu1205 melanoma cells for indicated time periods. HUVEC monolayer TER was measured as described under "Experimental Procedures." The time-dependent change in the electrical resistance of the HUVEC monolayer, which was stimulated with 80 ng/ml VEGF, served as a control. Values are mean ± S.E. from at least three independent experiments.

thrombin activity, resulted in a 52% reduction of the Lu1205/PFP-induced gap area (Fig. 2*F*). Concomitantly, inhibition of B-Raf(V600E), TF, and thrombin also reversed melanoma-mediated reduction of endothelial electrical resistance in PFP (Fig. 2*G*). To further demonstrate the role of tumor-derived thrombin on VE-cadherin junction disassembly, we silenced the primary thrombin receptor on endothelium, PAR-1, which upon binding to thrombin orchestrates downstream signaling leading to endothelial junction breakdown (35). siPAR-1 transfection reduced the endothelial PAR-1 mRNA level by 80% as assessed by PCR (Fig. 2*H*). PAR-1 knockdown markedly suppressed endothelial gap formation and barrier function loss induced by melanoma adhesion in the presence of PFP (Fig. 2, *H* and *I*). These results imply that

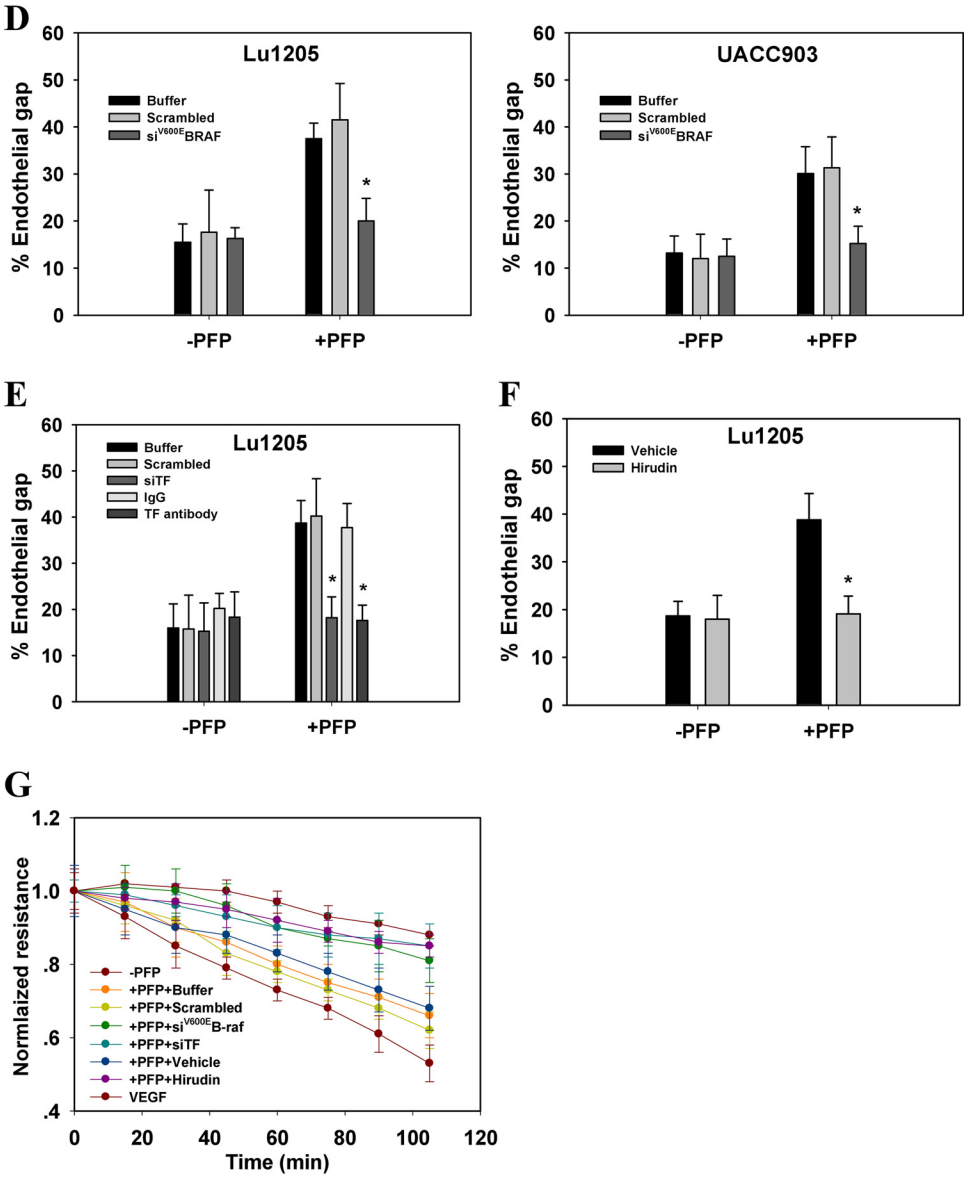


FIGURE 2—*continued*

thrombin signaling initiated by B-Raf(V600E)-positive melanoma contributes to loss of the VE-cadherin complex.

*Melanoma Reduced VE-cadherin-mediated Cell Adhesion by Triggering Thrombin Generation in Plasma*—Endothelial junction integrity is maintained by VE-cadherin-dependent cell-cell contact (25). The weakened cell-cell contacts lead to endothelial barrier function loss. To assess the effect of tumor-derived thrombin on VE-cadherin-mediated adhesion, HUVECs were co-cultured with melanoma cells before their affinity for VE-cadherin was assessed in the presence of melanoma/PFP culture medium. To simulate the VE-cadherin-mediated cell-cell contacts, VEC-Fc chimeric protein was used to coat dishes. In the absence of PFP, HUVECs adhered within 5 min to immobilized VEC-Fc and subsequently spread (Fig. 3*A*). No cells attached to the Fc-coated surface. After being co-cultured with metastatic melanoma cells (UACC903 and Lu1205), HUVEC adhesion to VEC-Fc was slightly reduced ($p > 0.05$). In contrast, cell adhesion was significantly diminished by adding PFP to HUVEC-melanoma co-culture. In addition, the magnitude of the reduction in cell adhesion was correlated with the metastatic potential of melanoma cells. PFP treatment augmented the suppressive effect of Lu1205 and UACC903 cells on HUVEC adhesion to the VEC-Fc-coated surface in a time-dependent manner (Fig. 3, *B* and *C*). A time course analysis revealed that enhanced adhesion was observed 10 min after plating (Fig. 3, *B* and *C*). Knockdown of B-Raf(V600E) or TF abrogated the inhibitory effect of Lu1205/PFP on HUVEC adhesion (Fig. 3*D*). A similar enhancement of cell adhesion to VE-cadherin was observed in HUVECs that were co-cultured with Lu1205 cells in the presence of hirudin. The suppression of VE-cadherin-mediated cell adhesion by Lu1205/PFP was also reversed by silencing PAR-1 in endothelial cells (Fig. 3*E*). Collectively, these results suggest that the down-regulation of VE-cadherin-mediated adhesiveness by melanoma contact in plasma is dependent on the activities of B-Raf(V600E) and thrombin.

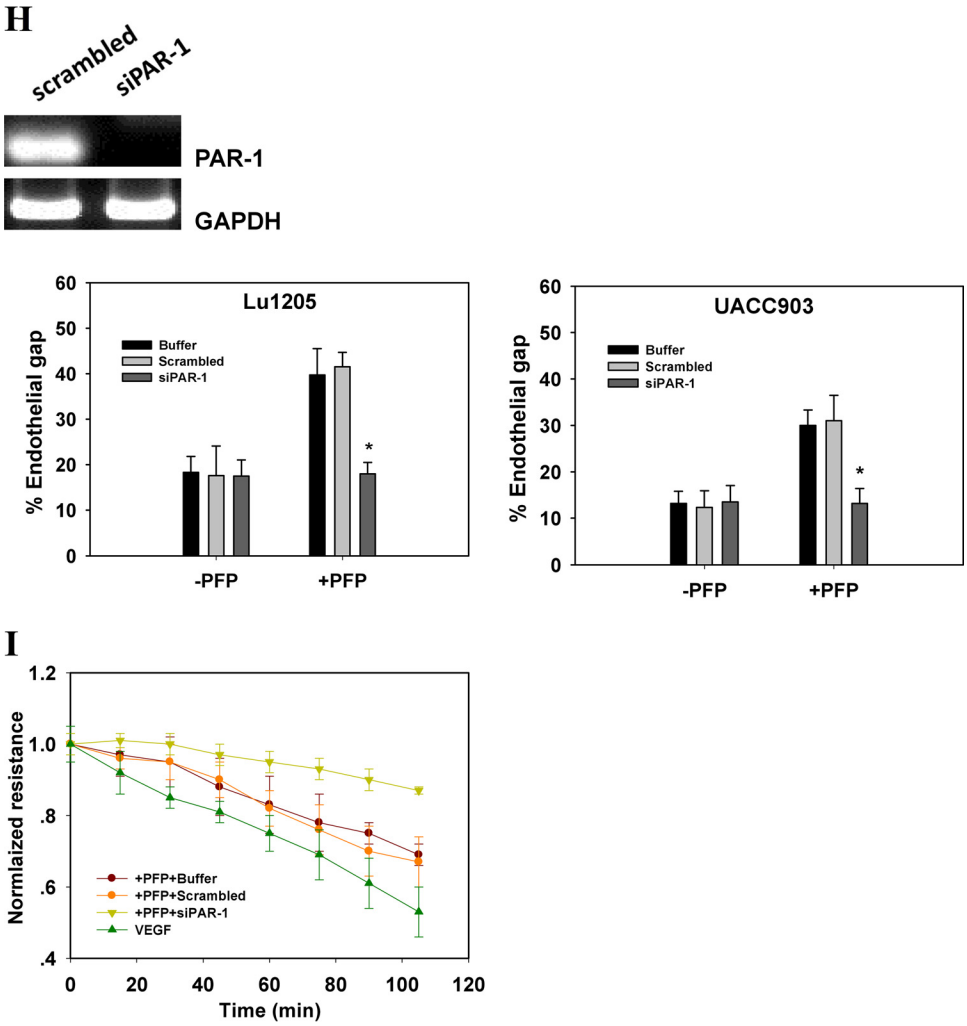


FIGURE 2—*continued*

*B-Raf(V600E) Overexpression Conferred on WM35 Cells the Ability to Promote Endothelial Junction Breakdown in a TF- and Thrombin-dependent Manner*—B-Raf(V600E) expression may lead to the activation of mitogen-activated protein kinase kinase/extracellular signal-regulated kinase 1/2 (MEK/ERK1/2), which promotes tumor growth and increases cell motility (29, 39). To exclude the possibility that the observed effect of B-Raf(V600E) on endothelial gap formation is a consequence of enhanced tumor growth and migration, we transfected a vector control, wild-type B-Raf or B-Raf(V600E), into non-metastatic WM35 cells that carry low levels of the B-Raf(V600E) mutant (Fig. 4*A*). Overexpression of B-Raf(V600E) but not wild-type B-Raf increased the expression of TF and enhanced melanoma-mediated endothelial junction dissociation in PFP (Fig. 4, *B* and *C*). The B-Raf(V600E)-mediated junction breakdown was reversed by knockdown of TF or inhibition of thrombin with hirudin (Fig. 4*C*). Similarly, knockdown of PAR-1 inhibited the effect of B-Raf(V600E) overexpression on endothelial junction breakdown. All of the results imply that the TF-thrombin/PAR-1 axis is essential for endothelial junction breakdown mediated by B-Raf(V600E)-positive melanoma cells.

*Tumor-derived Thrombin Triggered Phosphorylation of VE-cadherin and p120 and Ubiquitination of VE-cadherin*—AJ breakdown and VE-cadherin dimer dissociation are dependent on cytosolic domain phosphorylation of VE-cadherin (21). Nevertheless, there is a controversy in the literature with respect to which tyrosine residues of VE-cadherin are phosphorylated in response to thrombin treatment. Therefore, we attempted to identify the specific tyrosine residues of VE-cadherin phosphorylated upon melanoma contact in the presence of PFP. The basal phosphorylation levels of VE-cadherin at Tyr-658, Tyr-685, and Tyr-731 were low in HUVECs (Fig. 5*A*). Lu1205, UACC903, or A375M contact for 60 min resulted in a dramatic increase in VE-cadherin phosphorylation at Tyr-658, Tyr-685, and Tyr-731 in PFP (Fig. 5*A*). VE-cadherin phosphorylation was dependent on mutant B-Raf and TF activities, because it was suppressed by knockdown of B-Raf(V600E) or TF with siRNA (Fig. 5, *B* and *C*). Hirudin treatment attenuated VE-cadherin phosphorylation at Tyr-658, Tyr-685, and Tyr-731 in response to co-culture of Lu1205 and HUVEC with PFP (Fig. 5*D*). It has been suggested that VE-cadherin phosphorylation at Tyr-658 and Tyr-731 may reduce the affinity of VE-cadherin for p120 and promote p120 phosphorylation at the AJ complex (19). Therefore, we deter-

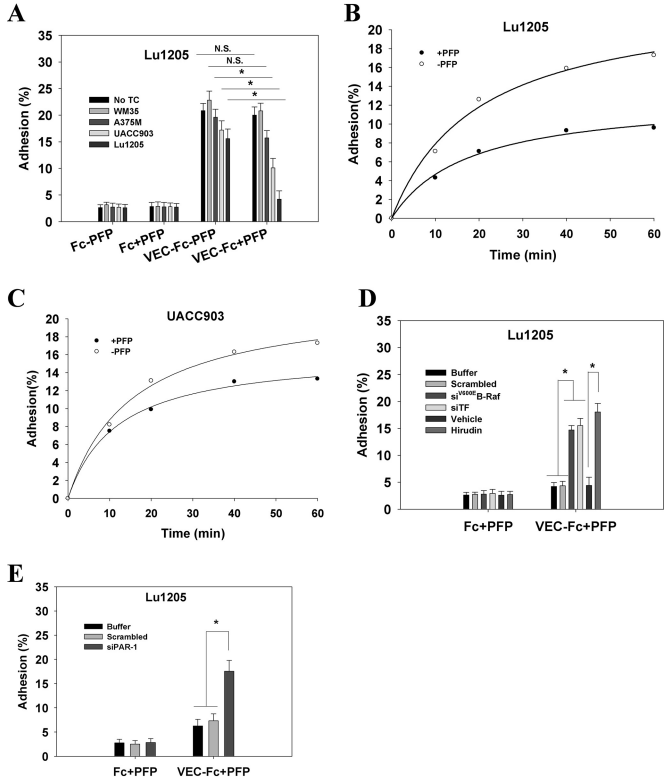


FIGURE 3. **Melanoma in the presence of PFP reduced VE-dependent HUVEC adhesion in a B-Raf(V600E)- and thrombin-dependent manner.** *A,* HUVEC monolayers were left alone or co-cultured with WM35, A375M, UACC903, or Lu1205 cells in the presence or absence of PFP. After being detached, HUVECs were plated onto a VEC-Fc- or Fc-coated dish in the presence of respective melanoma-HUVEC co-culture medium for 60 min. Cell adhesion was measured as described under "Experimental Procedures" and is shown as the percentage of adherent cells. Values are mean ± S.E. from three independent experiments. *B* and *C*, after co-culture with Lu1205 and UACC903 cells in the presence or absence of PFP, HUVECs were plated onto a VEC-Fc-coated dish for the time indicated. Cell adhesion is shown as the percentage of adherent cells. *D,* HUVECs were co-cultured with Lu1205 cells transfected with buffer, scrambled siRNA, siB-Raf(V600E), or siTF, or treated with vehicle or hirudin in the presence of PFP. Then they were assessed for adhesion activity as described in the legend to *A*. *E,* HUVECs transfected with buffer, scrambled siRNA, or siPAR-1 were co-cultured with Lu1205 cells in the presence of PFP. Then they were assessed for adhesion activity as described in the legend to *A*. *, $p < 0.05$. *N.S.,* not significant.

mined whether the changes in VE-cadherin phosphorylation induced by tumor-derived thrombin were associated with p120 phosphorylation. p120 phosphorylation levels were progressively elevated, which led to a progressive increase in melanoma metastatic potential as assessed by immunoprecipitation (Fig. 5*E*). Knockdown of B-Raf(V600E) or TF in Lu1205 or hirudin treatment significantly reduced p120 phosphorylation (Fig. 3, *F* and *G*).

Phosphorylated VE-cadherin undergoes clathrin-dependent endocytosis, which targets VE-cadherin for lysosomal degradation (19, 40–42). It has been suggested that p120 participates in VE-cadherin endocytosis (43). An increase in ubiquitination of the VE-cadherin cytoplasmic tail catalyzed by E3 ligase greatly enhances the trafficking of VE-cadherin into the lysosomal degradation process, thereby reducing the recycling of the protein from early endosomes to plasma membrane and decreasing the membrane abundance of VE-cadherin (44, 45). To demonstrate whether melanoma contact-mediated loss of the VE-cadherin complex requires VE-cadherin ubiquitination, we assessed the co-localization of VE-cadherin and Lys-63-linked ubiquitin, which is a marker for endocytosis. We found that Lu1205 adhesion in the presence of PFP increased internalized VE-cadherin in cytoplasmic vesicles that were associated with ubiquitination (Fig. 6*A*). Knockdown of B-Raf(V600E) or PAR-1 reduced Lu1205/PFP-induced VE-cadherin ubiquitination, supporting the concept that B-Raf(V600E)-mediated thrombin generation is required for VE-cadherin ubiquitination and internalization. Next, we isolated early endosomes and detected the levels of ubiquitinated VE-cadherin in early endosomes by immunoprecipitation. We found that the addition of PFP increased the amount of ubiquitinated VE-cadherin in early endosomes by 530 ± 85% ($p < 0.05$) (Fig. 6*B*). The effect of PFP on the ubiquitination of VE-cadherin was dependent on the B-Raf mutation and thrombin signaling, because knockdown of B-Raf(V600E) or PAR-1 prevented Lu1205/PFP-induced VE-cadherin ubiquitination in early endosomes. Therefore, ubiquitination-coupled VE-cadherin internalization is involved in melanoma-mediated loss of the endothelial VE-cadherin complex in the presence of PFP.

*Melanoma Contact-mediated Endothelial Focal Adhesion Assembly and Actin Polymerization Are Dependent on B-Raf (V600E) and PAR-1 Signaling*—We analyzed the dynamics of actin cytoskeleton and focal adhesion assembly, which have been shown to participate in thrombin-induced endothelial remodeling (46). In the presence of PFP, HUVECs exhibited thicker stress fibers than when PFP was absent. After co-culture with melanoma, the fibers traversed the cell body (Fig. 7*A*). In contrast, knockdown of B-Raf(V600E) in melanoma or silencing of PAR-1 in HUVECs altered the cytoskeletal morphology in HUVECs co-cultured with melanoma in PFP. In these cases, filamentous actin assembled around the cell periphery, with only a few thin stress fibers in the cell body. This implies that endothelial contractility may contribute to melanoma-induced endothelial junction breakdown.

By staining with paxillin, a focal adhesion marker, we showed that co-culture of melanoma and endothelium fostered focal adhesion assembly (Fig. 7*A*). Bright punctate focal adhesions, which were colocalized with the end of thick stress fibers, were formed in the HUVECs. Following knockdown of B-Raf(V600E) or PAR-1, focal adhesion staining dimmed. Small focal adhesions appeared at the cell periphery, and they almost disengaged with only thin stress fibers. Quantitative analysis of the average focal adhesion size and number in a cell revealed that melanoma contacts in the presence of PFP increased the size and number of focal adhesions in HUVECs in a B-Raf(V600E)- and PAR-1-dependent manner (Fig. 7, *B* and *C*).

*B-Raf(V600E) Expression Promoted Thrombin-mediated Melanoma TEM*—Because endothelial barrier loss and VE-cadherin disassembly may facilitate melanoma extravasation, we tested the possibility that the thrombogenic potential of melanoma cells is associated with melanoma TEM capacity. The presence of PFP significantly increased the TEM of B-Raf(V600E)-positive melanoma and A375M, UACC903, and Lu1205 cells (Fig. 8*A*). The number of migrating Lu1205 cells increased 2.9-fold in the +PFP group compared with the −PFP

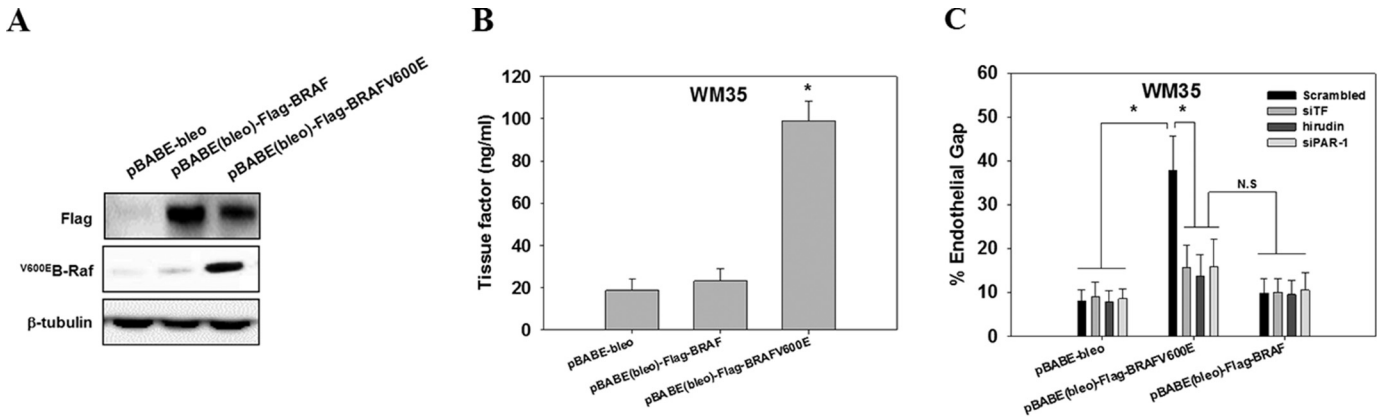


FIGURE 4. **Ectopic expression of B-Raf(V600E) in WM35 enhanced gap formation by increasing TF expression and thrombin generation.** *A,* WM35 cells were transfected with pBABE-bleo, pBABE(bleo)-FLAG-BRAF, or pBABE(bleo)-FLAG-BRAF(V600E) packed in retrovirus. Transfection efficiency was assessed by Western blotting with anti-FLAG and anti-B-Raf(V600E) antibodies. β-Tubulin serves as a loading control. *B,* WM35 cells transfected with pBABE-bleo, pBABE-(bleo)-FLAG-BRAF, or pBABE(bleo)-FLAG-BRAF(V600E) were assessed for membrane TF expression. TF measurement is described in legend to Fig. 1*B*. *, $p < 0.05$ compared with pBABE(bleo)-FLAG-BRAF. *C,* WM35 cells transfected with pBABE-bleo, pBABE(bleo)-FLAG-BRAF, or pBABE(bleo)-FLAG-BRAF(V600E) were co-transfected with scrambled siRNA or siTF or treated with hirudin. They were co-cultured with HUVECs transfected with scrambled siRNA or siPAR-1 for 60 min in the presence of PFP before endothelial gap formation was measured. Values are mean ± S.E. from three independent experiments. *, $p < 0.05$. *N.S.,* not significant.

group. Silencing B-Raf(V600E) or TF attenuated Lu1205 TEM capacity in the presence of PFP (Fig. 8, *B* and *C*). In contrast, Lu1205 TEM was unaffected by B-Raf(V600E) or TF depletion in the absence of PFP. Thrombin played an essential role in regulating Lu1205 extravasation, because inhibition of thrombin activity by pre-treating the plasma with hirudin significantly decreased the number of migrating Lu1205 cells ($p < 0.01$) (Fig. 8*D*). Thrombin treatment usually results in phosphorylation of p120-catenin at Ser-879, which dissociates p120-catenin from VE-cadherin and disrupts vascular integrity (1, 2, 47). To further corroborate the role of thrombin-induced junction breakdown in promoting melanoma migration, Ser-879 on p120 was mutated to alanine to generate a phosphorylation-defective p120 mutant (S879A-p120). The S879A-p120 mutant is constitutively associated with VE-cadherin even following thrombin stimulation. S879A-p120 was cloned into vectors containing a GFP tag and transfected into HUVECs. GFP-S879A-p120 was successfully transfected into HUVECs as measured by Western blotting (Fig. 8*E*). PFP-mediated Lu1205 TEM was attenuated when HUVECs were transfected with the mutant p120, although the basal Lu1205 migration in the absence of PFP was not susceptible to S879A-p120 transfection. Taken together, thrombin-induced endothelial barrier function loss promotes melanoma TEM via p120 phosphorylation at Ser-879.

*Melanoma Cells Took Paracellular Routes to Transmigrate in the Presence of PFP*—To determine the route and mechanism of melanoma cells' TEM, an *in vitro* transmigration model was used. Melanoma cells were loaded onto the apical side of an endothelial monolayer grown on a Matrigel-coated coverslip. Real time monitoring of melanoma TEM was conducted using a z-stack laser confocal microscopy system. Initially, melanoma randomly settled on the endothelial monolayer in different locations (junctional and nonjunctional sites). In the presence of PFP, within 5–10 min after coming into contact with endothelial cells, the melanoma cells plated on the endothelial monolayer started to spread (Fig. 9*A*). Some cells originally on nonjunctional sites migrated to junctional sites. 15–30 min later, the GFP·VE-cadherin complex was disrupted wherever it was in close proximity to any TC adhesions (Fig. 9*A*). Melanoma cells penetrated the gaps between the adjacent endothelial cells as revealed by examining an *x-z* cross-section (Fig. 9*B*). Cells completed the TEM process within 15–30 min, which was confirmed by their location beneath green endothelial lines (Fig. 9, *A* and *B*). After translocation, the cells became more flattened and elongated. Conversely, in the absence of PFP, melanoma cells were unable to migrate through the endothelial monolayer in the assay time frame (Fig. 9*A*).

Leukocytes undergo TEM via both the paracellular and transcellular routes (48). However, little is known about the routes melanoma cells follow. Confocal microscopy analysis of melanoma TEM routes revealed that in the absence of PFP 27.5% of melanoma cells underwent TEM (Fig. 9*C*). The addition of PFP enhanced melanoma paracellular TEM (67 ± 3% of total TCs). Of note, in the presence of PFP, cells taking transcellular routes only constituted 5.5% of the total TEM population. Knockdown of B-Raf(V600E) or PAR-1 caused a marked attenuation of paracellular TEM by melanoma cells, although transcellular TEM was unaffected (Fig. 9, *D* and *E*). The findings suggest that melanoma paracellular TEM is dictated by the activity of tumor-derived thrombin.

*Plasma Promoted Melanoma TEM under Shear Conditions*—Flow-regulated cancer migration plays an important role in tumor metastasis (1). To evaluate the effect of PFP treatment on cancer migration under hydrodynamic conditions, we used a flow migration device (16, 28, 49). At shear stresses of 2 and 4 dynes/cm$^2$, Lu1205 and UACC903 cells transmigrated more efficiently in the presence of PFP than in the absence of PFP ($p < 0.05$) (Fig. 10, *A* and *B*). At 2 and 4 dynes/cm$^2$, knockdown of B-Raf(V600E) or PAR-1 significantly reduced PFP-mediated Lu1205 and UACC903 TEM (Fig. 10, *C–F*). At 4 dynes/cm$^2$, B-Raf(V600E) and PAR-1 depletion resulted in 52- and 61-fold reductions in Lu1205

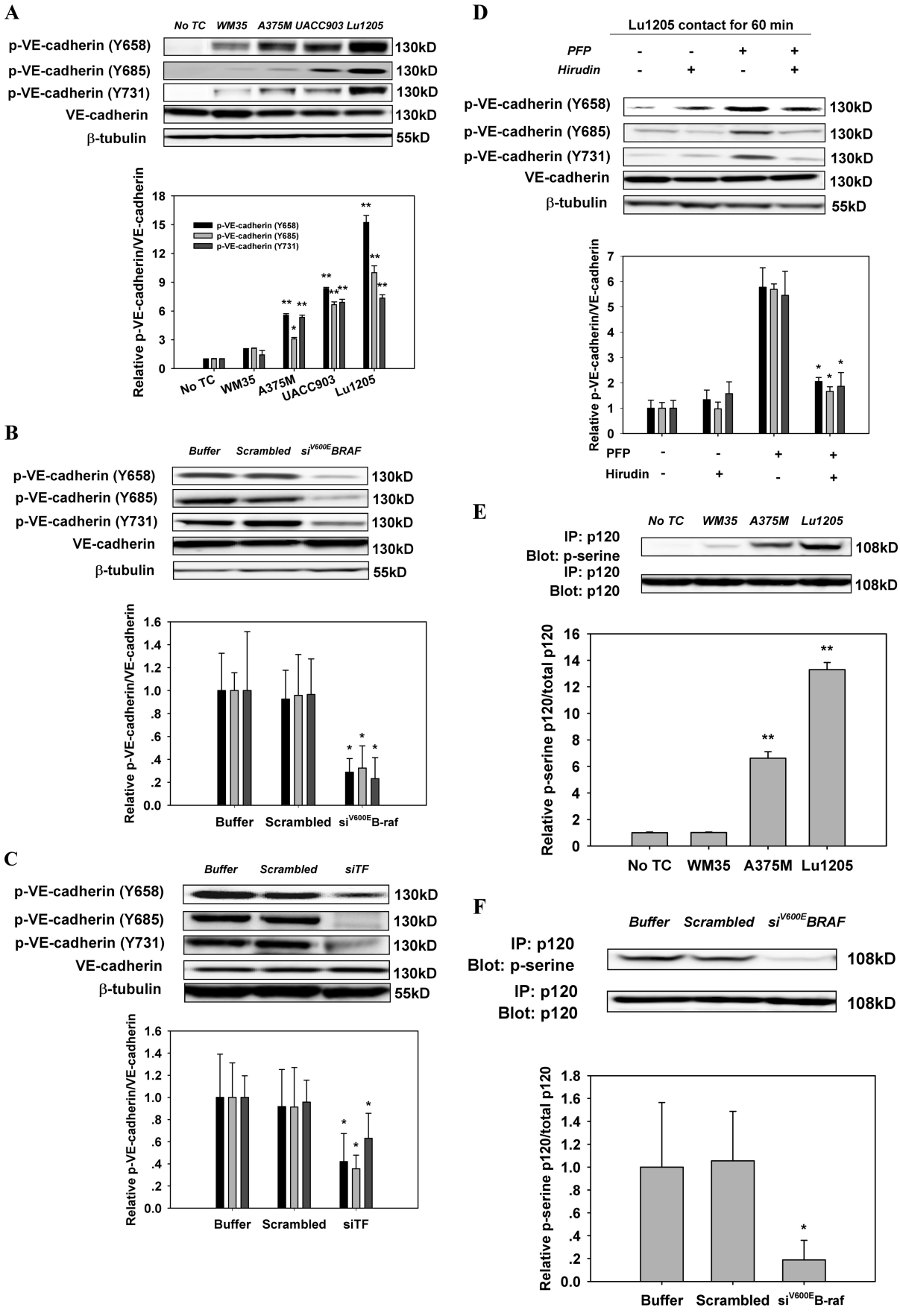
A
No TC WM35 A375M UACC903 Lu1205
p-VE-cadherin (Y658)
p-VE-cadherin (Y685)
p-VE-cadherin (Y731)
VE-cadherin
β-tubulin
130kD
130kD
130kD
130kD
55kD
Relative p-VE-cadherin/VE-cadherin
p-VE-cadherin (Y658)
p-VE-cadherin (Y685)
p-VE-cadherin (Y731)
No TC WM35 A375M UACC903 Lu1205
B
Buffer Scrambled siV600EBRAF
p-VE-cadherin (Y658)
p-VE-cadherin (Y685)
p-VE-cadherin (Y731)
VE-cadherin
β-tubulin
130kD
130kD
130kD
130kD
55kD
Relative p-VE-cadherin/VE-cadherin
Buffer Scrambled siV600EB-raf
C
Buffer Scrambled siTF
p-VE-cadherin (Y658)
p-VE-cadherin (Y685)
p-VE-cadherin (Y731)
VE-cadherin
β-tubulin
130kD
130kD
130kD
130kD
55kD
Relative p-VE-cadherin/VE-cadherin
Buffer Scrambled siTF
D
Lu1205 contact for 60 min
PFP - - + +
Hirudin - + - +
p-VE-cadherin (Y658)
p-VE-cadherin (Y685)
p-VE-cadherin (Y731)
VE-cadherin
β-tubulin
130kD
130kD
130kD
130kD
55kD
Relative p-VE-cadherin/VE-cadherin
PFP - - + +
Hirudin - + - +
E
No TC WM35 A375M Lu1205
IP: p120
Blot: p-serine
IP: p120
Blot: p120
108kD
108kD
Relative p-serine p120/total p120
No TC WM35 A375M Lu1205
F
Buffer Scrambled siV600EBRAF
IP: p120
Blot: p-serine
IP: p120
Blot: p120
108kD
108kD
Relative p-serine p120/total p120
Buffer Scrambled siV600EB-raf

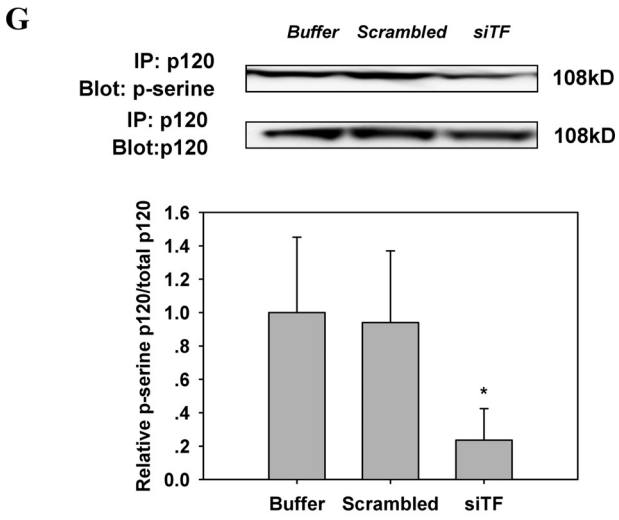


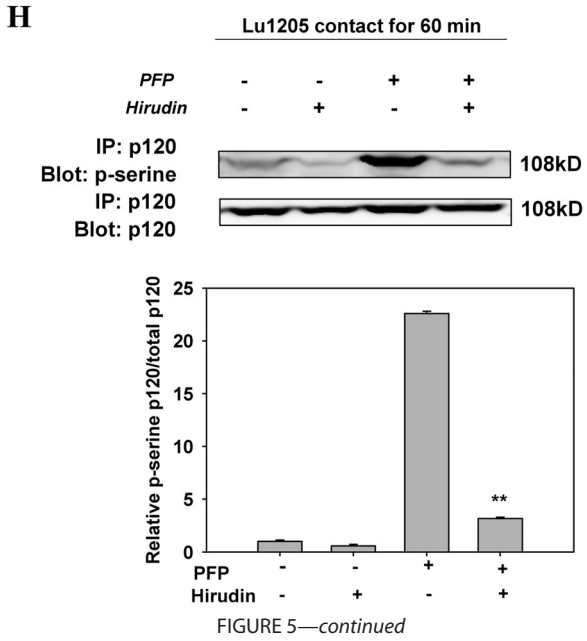


FIGURE 5—*continued*

migration, respectively (Fig. 10, *C* and *E*). The results indicate that melanoma TEM under shear conditions requires a functional B-Raf(V600E)/TF/thrombin axis.

## Discussion

Most deaths caused by melanoma occur from disseminated and drug-resistant tumors disrupting major organ function (15, 49, 50). Therefore, understanding the molecular mechanisms that regulate metastasis is crucial to developing new therapeutic strategies to treat melanoma metastases. In this study, we provided evidence that the presence of a B-Raf(V600E) mutant in melanoma is associated with TF overexpression and aberrant thrombin generation. In addition, our findings revealed that tumor-derived thrombin is involved in promoting the loss of VE-cadherin junction integrity during melanoma TEM, which is mediated by phosphorylation of VE-cadherin and p120, and ubiquitination of VE-cadherin. In the presence of plasma, melanoma takes paracellular routes to achieve TEM. To the best of our knowledge, it is the first study to relate tumor-derived thrombin with endothelial junction breakdown.

The proto-oncogene B-Raf has an activating mutation for a valine-to-glutamic acid change at residue 600 rendering it constitutively active in a majority of melanoma cells (9, 12). The V600E mutation is thought to mimic phosphorylation, leading to constitutive ERK activation (15). Targeting B-Raf(V600E) reduces tumor lung entrapment by decreasing the secretion of tumor IL-8 and interrupting ICAM-1-$\beta_2$ integrin binding of tumor cells to the endothelium, which is mediated by neutrophils in circulation (16). Furthermore, the roles of B-Raf(V600E) in inducing MMP-1 secretion and activating adjacent fibroblasts in the tumor microenvironment have been demonstrated (51). In this study, we showed a mechanistic link between B-Raf(V600E), TF expression, thrombin production, and endothelial junction breakdown. Although the role of B-Raf(V600E) in mediating tumor growth has been established (30, 52), it is unlikely that B-Raf(V600E)-mediated endothelial gap formation and melanoma extravasation are related to the functions of B-Raf(V600E) in tumor growth and cell cycle progression, because the time scale of endothelial gap formation

FIGURE 5. **Inhibition of the activities of B-Raf(V600E), TF, or thrombin reversed the increase of phosphorylation of VE-cadherin and p120-catenin in endothelium caused by melanoma contacts in plasma.** *A,* co-culture between B-Raf(V600E)-positive melanoma and HUVECs promoted phosphorylation of VE-cadherin at tyrosine 658, 685, and 731. Confluent HUVEC monolayers were serum-starved for 12 h. They were either left alone (*no TC*) or co-cultured with $1 \times 10^6$ melanoma cells (WM35, A375M, UACC903, or Lu1205) in the presence of PFP for 60 min before Western blot analysis. *B,* silencing B-Raf(V600E) suppressed co-culture-induced tyrosine phosphorylation of VE-cadherin. HUVECs were subjected to Western blot analysis after being co-cultured with $1 \times 10^6$ Lu1205 melanoma cells transfected with buffer, scrambled siRNA, or B-Raf(V600E) siRNA in the presence of PFP for 60 min. *C,* silencing TF suppressed co-culture-induced tyrosine phosphorylation of VE-cadherin. HUVECs were subjected to Western blot analysis after being co-cultured with $1 \times 10^6$ Lu1205 melanoma cells transfected with buffer, scrambled siRNA, or TF siRNA in the presence of PFP for 60 min. *D,* hirudin suppressed co-culture-induced tyrosine phosphorylation of VE-cadherin. HUVECs were subjected to Western blot analysis after being co-cultured with $1 \times 10^6$ Lu1205 melanoma cells in the presence or absence of PFP with or without 40 units/ml hirudin for 60 min. *E,* serine phosphorylation of p120-catenin was triggered by melanoma contacts in the presence of PFP. HUVECs were left alone (*no TC*) or co-cultured with $1 \times 10^6$ melanoma cells (WM35, A375M, or Lu1205) in the presence of PFP for 60 min. HUVECs were subjected to immunoprecipitation (*IP*). *F,* serine phosphorylation of p120-catenin was suppressed by B-Raf(V600E) silencing. HUVECs were co-cultured with buffer, scrambled siRNA, or B-Raf(V600E) siRNA-transfected Lu1205 cells in the presence of PFP. HUVECs were subjected to immunoprecipitation. *G,* serine phosphorylation of p120-catenin was suppressed by TF silencing. HUVECs were co-cultured with buffer, scrambled siRNA, or TF siRNA-transfected Lu1205 cells in the presence of PFP. HUVECs were subjected to immunoprecipitation. *H,* serine phosphorylation of p120-catenin was abolished by hirudin treatment. HUVECs were subjected to immunoprecipitation after being co-cultured with $1 \times 10^6$ Lu1205 melanoma cells in the presence or absence of PFP with or without 40 units/ml hirudin for 60 min. For Western blot analysis, HUVECs were lysed and subjected to blotting using phospho-VE-cadherin-specific antibodies (Tyr(P)-658, Tyr(P)-685, and Tyr(P)-731). VE-cadherin and $\beta$-tubulin served as loading controls. For immunoprecipitation, precipitated proteins were analyzed by immunoblotting with an antibody against phosphoserine. The same blot was stripped and then reprobed with an antibody to p120-catenin. Relative VE-cadherin phosphorylation and p120 phosphorylation for densitometric analysis are shown below each blot. Values are mean ± S.E. *, $p < 0.05$; **, $p < 0.01$ compared with control. All results are representative of at least three independent experiments.

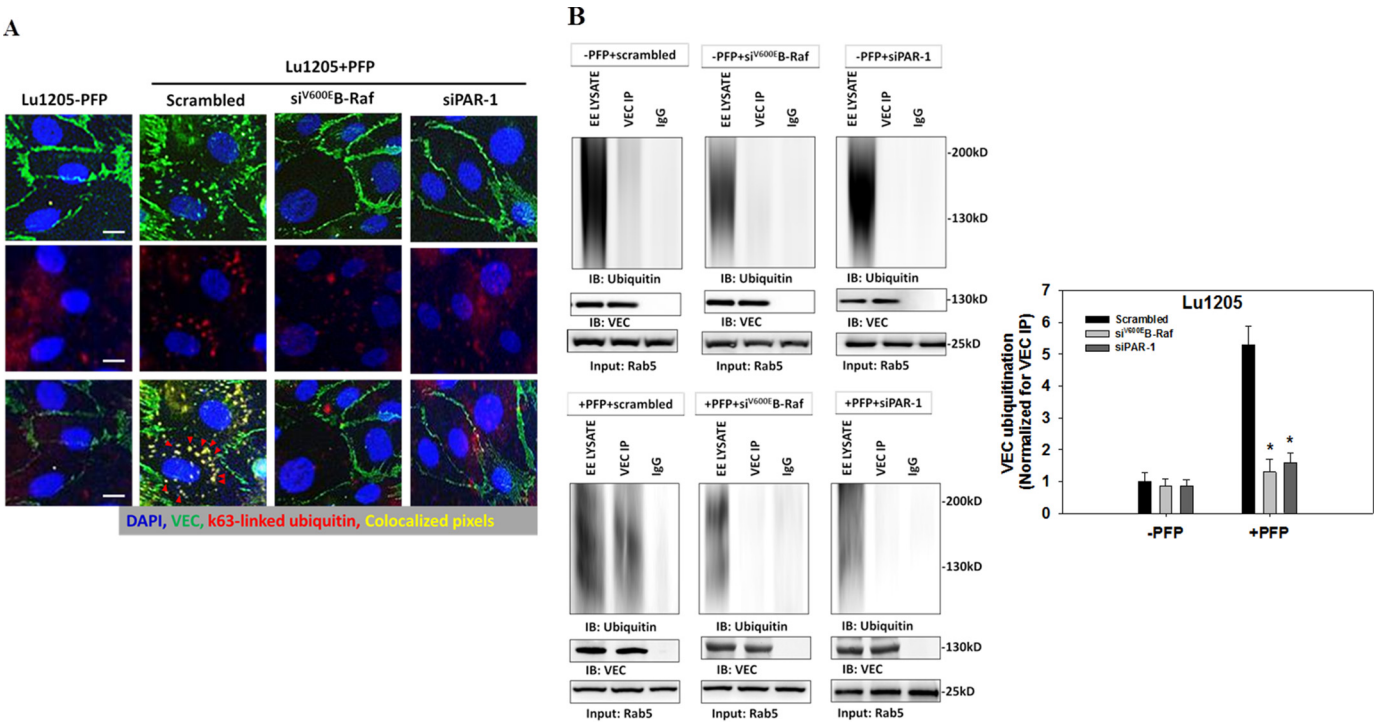


FIGURE 6. **Knockdown of B-Raf(V600E) or PAR-1 reduced melanoma-induced endothelial VE-cadherin ubiquitination and endocytosis in plasma.** HUVECs transfected with scrambled siRNA or siRNA against PAR-1 were incubated with 300 $\mu$M chloroquine for 3 h. Then they were co-cultured with Lu1205 cells transfected with scrambled siRNA or siRNA against B-Raf(V600E) in the presence or absence of PFP for 60 min. *A,* Lu1205/PFP-induced VE-cadherin internalization (*red staining*) and co-localization in intracellular vesicles with K63-linked ubiquitin (*green staining*) in HUVECs were abrogated following siB-Raf(V600E) or siPAR-1 transfection. Pixels representing ubiquitin and VE-cadherin colocalization are highlighted in *yellow*. *Red arrowheads* point to internalized VE-cadherin. Data are representative of three independent experiments. *Bar,* 10 $\mu$m. *B,* VE-cadherin (*VEC*) was immunoprecipitated (*IP*) from the early endosome fraction, and ubiquitinated VE-cadherin was detected with Western blotting (*IB*) using an anti-ubiquitin antibody (FK2, Millipore). *EE LYSATE*, lysate from early endosome preparation. *VEC IP*, immunoprecipitated VE-cadherin. *IgG,* immunoprecipitation using an IgG isotype control. Rab5 protein was probed to validate the status of early endosomes and ensure equal loading across samples. Representative blots from three independent experiments are shown. *Bottom panel* is a quantitation of ubiquitinated VE-cadherin in different cases. Data were normalized against the amount of VE-cadherin immunoprecipitated from early endosome preparation. Values are mean ± S.E. *, $p < 0.05$ compared with Lu1205/PFP/Scrambled.

and melanoma extravasation is short compared with that of cell growth, which normally requires gene expression changes. In addition, inhibition of TF and thrombin signaling reversed the effect of the ectopic expression of B-Raf(V600E) in a non-metastatic cell line, WM35, on endothelial junction breakdown (Fig. 4*C*). Therefore, the observed melanoma-mediated endothelial junction dissociation is the direct consequence of B-Raf(V600E)-mediated thrombogenesis.

TF has been implicated in mediating tumor cell survival, growth, invasiveness, and angiogenesis. TF overexpression is associated with the hypercoagulable status of cancer patients and poor prognosis. Down-regulation of TF expression results in suppression of the ERK and PI3K/Akt pathways (6, 53). Similar to our findings about the function of B-Raf(V600E) in TF expression, kinase suppressor of Ras-1 (KSR1), a scaffold protein involved in EGF receptor signaling in tumor cells, was found to up-regulate TF expression, increasing tumor aggressiveness (54). It was also suggested that factor VII ectopically synthesized by TF-expressing cells can trigger factor X activation and tumor cell invasion (55). For thrombin generation, TF needs to engage with factor VIIa and catalytically activate factor X, which can convert prothrombin to thrombin (4). It was reported that tumor-mediated thrombin generation requires functional prothrombinase assembly on cell surfaces consisting of factor Xa, factor Va, and calcium. In line with this, our data showed that in the absence of PFP, TF expression on melanoma was no longer a determinant for endothelial junction breakdown or for tumor TEM.

B-Raf(V600E) can promote IL-8 secretion from tumor cells, which may cause endothelial activation (16, 56). Some tumor cells express very late antigen-4 (VLA-4), leukocyte function-associated antigen-1 (LFA-1), and E-selectin ligands that can bind to receptors on endothelium to trigger VE-cadherin homodimer disassembly (23, 57). Importantly, colon cancer adhesion to E-selectin activates ERK, which triggers Src-mediated dissociation of the VE-cadherin·$\beta$-catenin complex (57). However, in this study, without plasma, melanoma was unable to induce VE-cadherin junction breakdown (Fig. 2, *A* and *B*). In addition, knockdown of CD44 and VLA-4 on melanoma cells did not reduce gap formation (data not shown). Therefore, receptor-mediated cell adhesion is not required for melanoma/PFP-induced AJ breakdown. This may be explained by the fact that during tumor TEM, the time scale of tumor contact with endothelium is short, especially in the face of shearing forces (50, 58, 59). Therefore, within the short contact period (60 min), cytokine and receptor-ligand engagement-initiated signaling may not be strong enough to induce gap formation. Endogenous thrombin in the tumor microenvironment is critical for mediating potent and rapid endothelial responses. Nevertheless, melanoma cells have to be brought in close apposi-

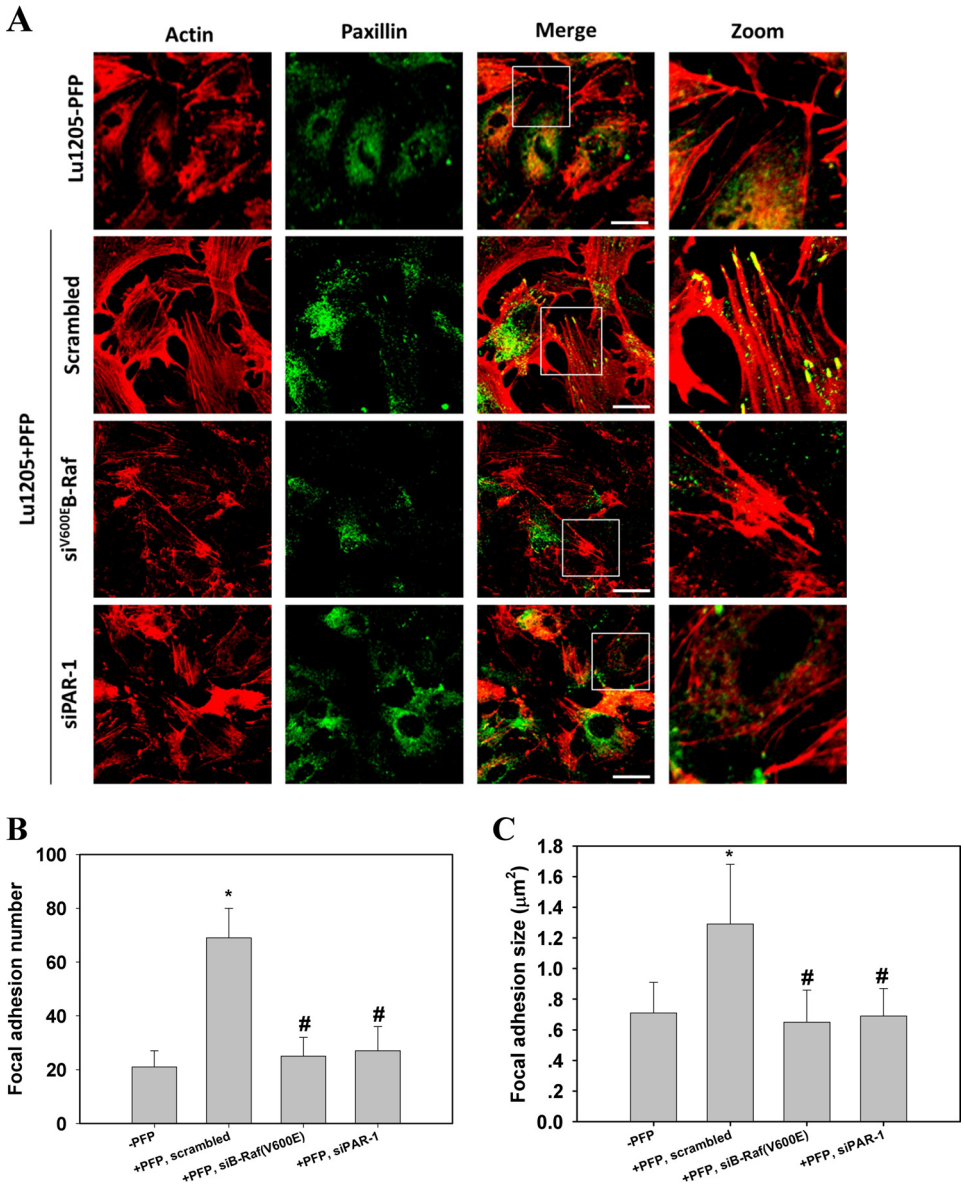


FIGURE 7. **Endothelial stress fiber formation and focal adhesion assembly induced by melanoma contacts were suppressed after knockdown of B-Raf(V600E) or PAR-1.** *A,* HUVEC untransfected or transfected with siRNA against PAR-1 were co-cultured with melanoma cells transfected with scrambled siRNA or siRNA against B-Raf(V600E) in the presence or absence of PFP. HUVECs were stained with rhodamine-phalloidin and paxillin antibody. The *right panel* shows magnified views of the *boxed area* in the merged images. *Bar* = 10 $\mu$m. (*Green* = paxillin and *red* = F-actin.) *B* and *C,* quantification of the average number and size ($\mu m^2$) of paxillin-containing focal adhesions in HUVECs using ImageJ software. 12 cells were analyzed per condition in each experiment. Values are mean ± S.E. *, $p < 0.05$ compared with −PFP; #, $p < 0.05$ compared with scrambled, +PFP.

tion of the endothelial junction to exert their effects, as focal loss of VE-cadherin complexes was only seen at the sites of melanoma contact (Fig. 2*A*). It is likely that AJ breakdown requires signaling triggered by threshold concentrations of thrombin. In thrombosis, cell membrane-associated prothrombinase cleaves prothrombin to release active thrombin, which is subject to diffusive and convective transport via intrathrombic permeation (60). Under physiological flow conditions, the generation and subsequent transport of thrombin from TF-rich sites play important roles in regulating the rate and extent of endothelial activation. Tumor cells may generate local thrombin concentration gradients that are determined by thrombin diffusivity so that its effect on endothelial gap formation is decreased with increasing distance from the tumor cell surface (61).

An intact endothelial monolayer is maintained by VE-cadherin homophilic adhesion at the endothelial boundary (62). It has been suggested that thrombin rapidly increases endothelial permeability, inducing redistribution of junctional proteins, including VE-cadherin, p120, and $\beta$-catenin (17, 21). A transient and focal disruption of the VE-cadherin complex was observed during leukocyte TEM (63, 64). This study showed that melanoma cells follow the paradigm of leukocyte TEM, mediating transient and focal reorganization of junctional proteins. This process may be activated by intracellular kinases, such as Src and protein kinase C, which are located downstream of the thrombin/PAR-1 association, to down-regulate endothelial barrier function (34, 36, 47). Phosphorylation of VE-cadherin on different tyrosine residues by these kinases regulates

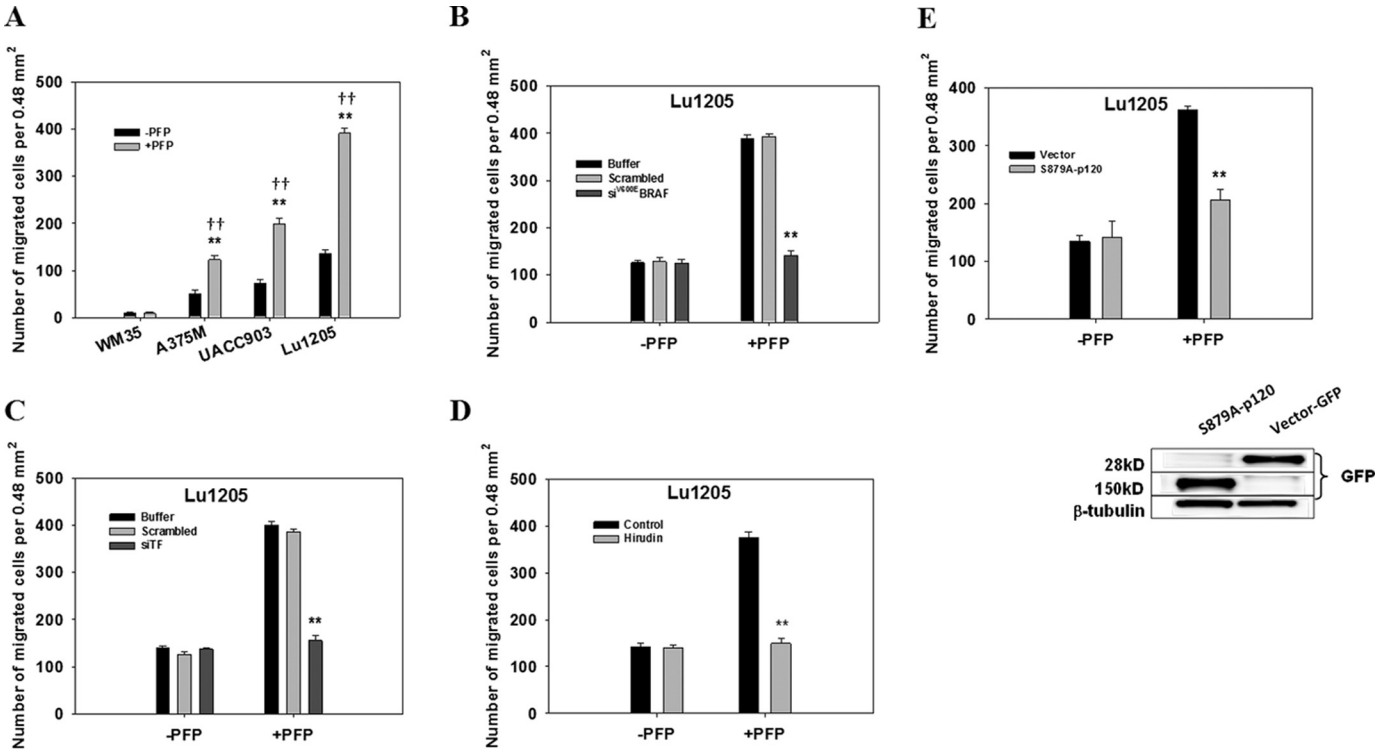


FIGURE 8. **Inhibition of B-Raf(V600E)-mediated thrombin generation attenuated melanoma TEM.** *A,* melanoma TEM was significantly increased by plasma treatment. The migration of $1 \times 10^6$ WM35, A375M, UACC903, or Lu1205 melanoma cells across the HUVEC monolayer was assessed in a Boyden chamber in the presence or absence of PFP. **, $p < 0.01$ compared with −PFP; ††, $p < 0.01$ compared with no TC control. Values are mean ± S.E. *B–D,* silencing B-Raf(V600E) (*B*) or TF (*C*) or inhibition of thrombin with hirudin (*D*) dramatically reduced PFP-induced Lu1205 cell TEM. **, $p < 0.01$ compared with control cases. Values are mean ± S.E. *E,* p120-catenin S879A mutation attenuated PFP-induced Lu1205 cell TEM. **, $p < 0.01$ compared with control cases. Values are mean ± S.E. Immunoblots show the expression of S879A-p120 (150 kDa) in HUVECs. β-Tubulin served as a loading control.

endothelial permeability and leukocyte TEM in different ways (65). Previous studies indicated that tyrosine phosphorylation of VE-cadherin is insufficient to promote an increase in endothelial permeability, and that VE-cadherin dephosphorylation is coupled with junction breakdown (18, 34). In this study, we found that endothelial gap formation is accompanied by VE-cadherin phosphorylation at tyrosine residues Tyr-658, Tyr-685, and Tyr-731, suggesting that VE-cadherin phosphorylation at these residues may contribute to focal AJ disruption induced by tumor-derived thrombin. In agreement with this, Tyr-658 and Tyr-731 of VE-cadherin were reported to modulate the affinity of VE-cadherin for β-catenin and p120 upon thrombin challenge (19). Phosphorylation at Tyr-658 and Tyr-731 may displace β-catenin and p120 from VE-cadherin and result in VE-cadherin internalization. The endocytosed VE-cadherin is subsequently ubiquitinated, recruited into early endosomes, and targeted for lysosomal degradation (20). In accordance with this, we found that VE-cadherin is ubiquitinated and sorted into Rab5-positive early endosomes, and disrupting the B-Raf(V600E)/TF/thrombin axis attenuates ubiquitin-coupled VE-cadherin endocytosis. Several studies have suggested that disruption of p120-catenin binding to VE-cadherin can result in cadherin internalization and degradation (43, 66). p120 dissociation from VE-cadherin leads to loss of VE-cadherin homodimer binding and junction disassembly. The roles of p120 phosphorylation at AJs in melanoma TEM were verified by using a phosphodeficient S879A-p120 mutant that has been shown to prevent an increase in endothelial permeability induced by thrombin/PAR-1 association (47). Overexpression of this construct in endothelium inhibited PFP-mediated melanoma TEM, suggesting the vital function of p120 in melanoma extravasation. It is of interest to identify the upstream kinases regulating VE-cadherin and p120 phosphorylation and the ubiquitin-ligase responsible for VE-cadherin ubiquitination, albeit such questions are beyond the scope of this study. They will be the focus of our future studies.

Vascular endothelial gap formation consists of two inter-related processes as follows: "unzipping" of the VE-cadherin homodimer complex mediated by phosphorylation of VE-cadherin, p120, β-catenin, and α-catenin; and "pulling" of the endothelial membrane by actomyosin machinery. It has been suggested that tumor adhesion or thrombin stimulation induces endothelial p38 phosphorylation, which promotes myosin light chain phosphorylation-mediated formation of stress fibers, although the activation of ERK by E-selectin initiates the activation of Src kinase and dissociation of the VE-cadherin·β-catenin·p120 complex (57). The loss of the VE-cadherin·β-catenin·p120 complex destabilizes actin and leads to actin remodeling and cell retraction (19). Thrombin may induce endothelial retraction by remodeling the cytoskeleton (67). In agreement with these observations, we showed that melanoma contact in the presence of plasma induces endothelial stress fiber formation and focal adhesion assembly. Knockdown of B-Raf(V600E) or PAR-1 impairs the ability of melanoma to mediate these phenotype changes.

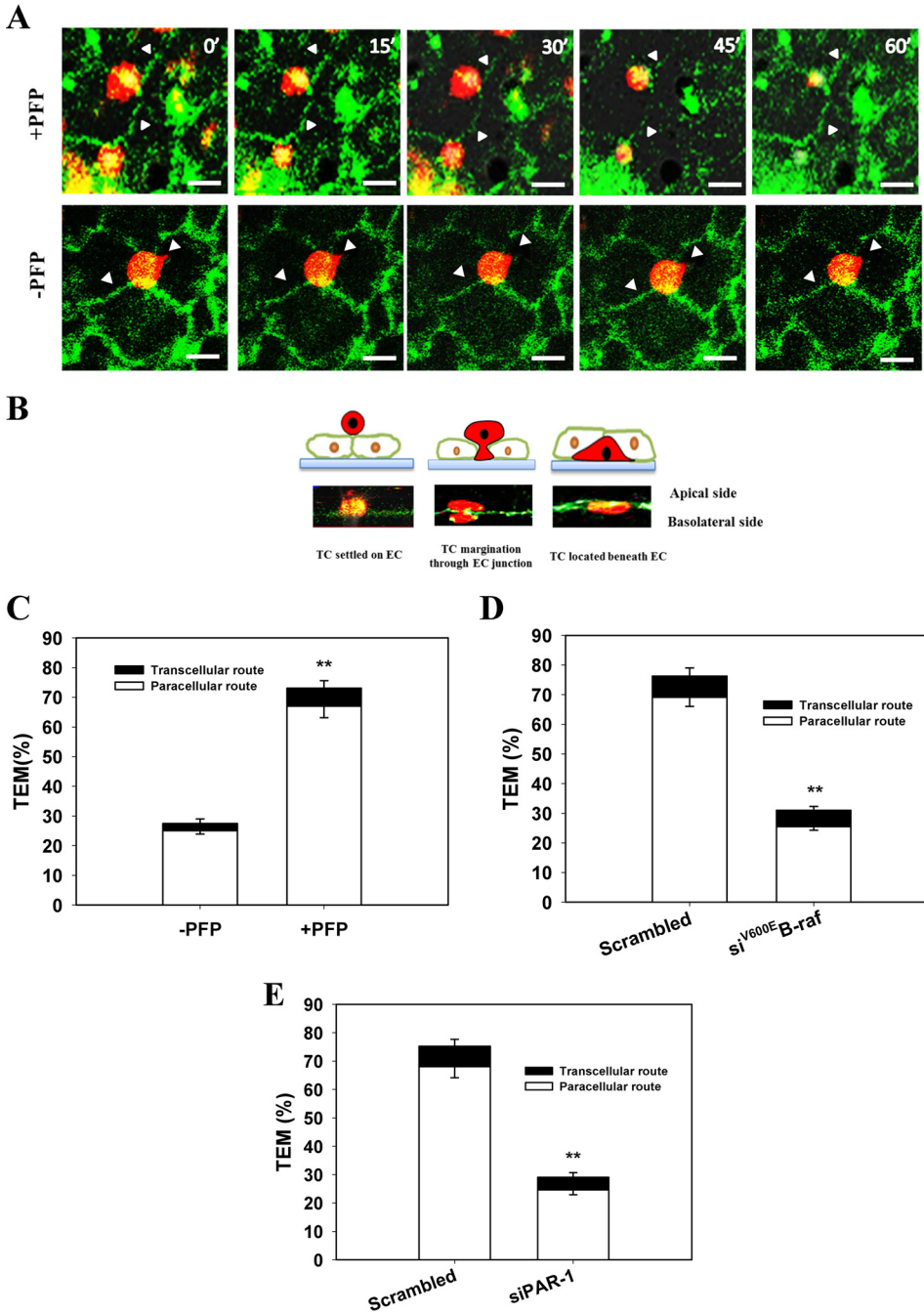


FIGURE 9. **Melanoma cells underwent TEM in plasma via paracellular routes.** *A,* confocal images show the migration of melanoma cells from the apical side to the basolateral side of HUVECs in the presence or absence of PFP. The locations of the same Lu1205 cells were captured at 0, 15, 30, 45, and 60 min of TEM. Lu1205 cells were stained with DiI before being seeded on a HUVEC monolayer, which was transfected with GFP-VE-cadherin. *B, X/Z* cross-sections of images of transmigrating Lu1205 cells. Micrographs show the stages of TEM as follows: TC settlement on EC; TC margination through EC; and TC localization beneath EC. The schematic drawing above each image represents the stage of TEM shown in the micrograph. *Bar,* 10 $\mu$m. *White arrowheads* indicate junctional sites. *C,* percentage of adherent Lu1205 cells taking transcellular and paracellular routes for TEM in the presence or absence of PFP. *D,* percentage of buffer, scrambled siRNA, or siB-Raf(V600E)-transfected Lu1205 cells taking transcellular and paracellular routes for TEM in the presence of PFP. *E,* percentage of Lu1205 cells taking transcellular and paracellular routes for migrating across buffer, scrambled siRNA, or siPAR-1-transfected HUVEC monolayer in the presence of PFP. Values are mean ± S.E. from three independent experiments. **, $p < 0.01$ compared with control cases.

Therefore, the observed gap formation in this study may largely depend on actin remodeling and cell retraction in response to the local release of thrombin from melanoma cells.

Transmigrating leukocytes pass through the endothelial monolayer via both paracellular (through the interendothelial junctions) and transcellular (through endothelial cup structure formation) routes. It has been suggested that like leukocytes, breast cancer cells are able to use both paracellular and transcellular transmigration routes (68). Here, we showed that PFP-dependent melanoma TEM occurs mainly via the paracellular route. This TEM behavior may be a unique melanoma characteristic, which is controlled by melanoma-derived thrombin signaling. Quantification of gap sizes was

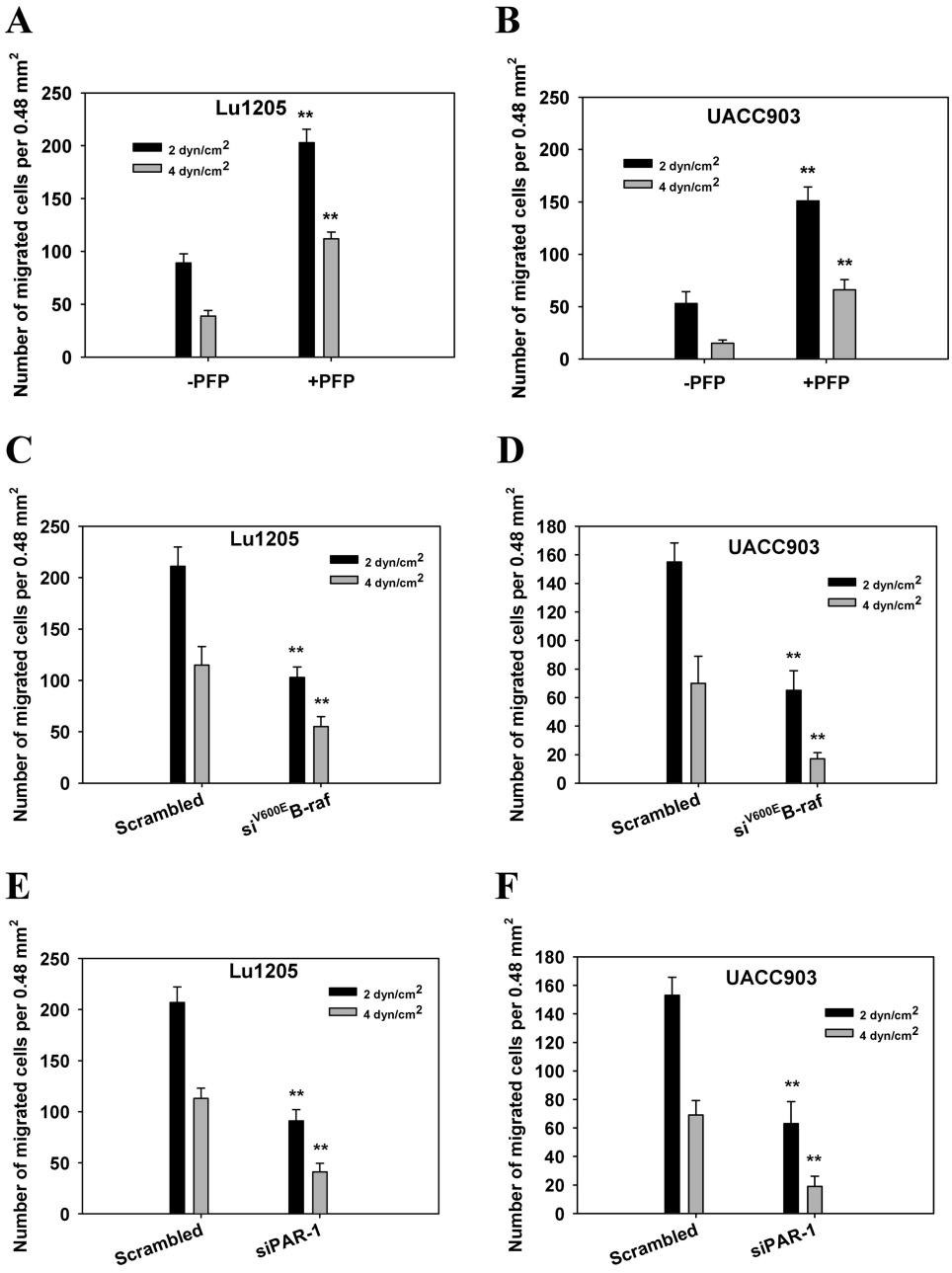


FIGURE 10. **Knockdown of B-Raf(V600E) or PAR-1 reduced melanoma TEM under shear conditions.** *A*, Lu1205; *B;* UACC903 TEMs were measured at a shear stress of 2 or 4 dynes/cm$^2$ in the presence or absence of PFP. *C* and *D,* scrambled siRNA or siB-Raf(V600E)-transfected Lu1205 (*C*) and UACC903 (*D*) TEMs were measured at a shear stress of 2 or 4 dynes/cm$^2$ in the presence of PFP. *E* and *F,* transmigrations of Lu1205 (*E*) or UACC903 (*F*) across scrambled siRNA or siPAR-1-transfected HUVECs were measured at a shear stress of 2 or 4 dynes/cm$^2$ in the presence of PFP. Values are mean ± S.E. from three independent experiments. **, $p < 0.01$ compared with control.

used in this study as a means of assessing the effect of melanoma contact on AJ breakdown (69, 70). Tumor transmigration and associated AJ breakdown are not synchronized events, but happen continuously. The disrupted VE-cadherin complex quickly reseals after tumor passage. Therefore, it is impossible to determine the effect of melanoma on AJ breakdown during real time migration assays. Quantification of gap size after melanoma-endothelium co-culture remains the most suitable approach for this purpose. The observed gaps are highly relevant to melanoma TEM, as it was observed that melanoma cells frequently take nearby *de novo*-formed gaps for TEM. In addition, focal and transient loss of the VE-cadherin complex is strongly correlated with melanoma transmigration potentials.

In conclusion, our study revealed that melanoma-derived thrombin plays essential roles in regulating endothelial junction integrity and tumor transmigration. In a tumor microenvironment, tumor-bound TF triggers production of thrombin, which upon binding to PAR-1 induces VE-cadherin phosphorylation at Tyr-658, Tyr-685, and Tyr-731 and p120 phosphorylation at Ser-879. These phosphorylation events ultimately result in dissociation of the VE-cadherin·p120 complex, loss of VE-cadherin homodimer binding, and VE-cadherin ubiquitination, thereby inducing endothelial gap formation and tumor transmigration.

This study provides a mechanistic basis for therapeutically targeting B-Raf(V600E) and TF to inhibit melanoma metastasis.

*Author Contributions*—P. Z. and C. D. conceived and coordinated the study and wrote the paper. P. Z., S. F., H. F. Z., Q. R., H. Y. B., and C. L. F. designed, performed, and analyzed the experiments. G. T. L. and H. Y. W. provided technical assistance and contributed to the preparation of the figures. All authors reviewed the results and approved the final version of the manuscript.

*Acknowledgment—We thank A. Reynolds (Vanderbilt University, Nashville, TN) for providing S879A-p120 plasmid.*

## References


1. Konstantopoulos, K., and Thomas, S. N. (2009) Cancer cells in transit: the vascular interactions of tumor cells. *Annu. Rev. Biomed. Eng.* **11,** 177–202
2. Wirtz, D., Konstantopoulos, K., and Searson, P. C. (2011) The physics of cancer: the role of physical interactions and mechanical forces in metastasis. *Nat. Rev. Cancer* **11,** 512–522
3. Biggerstaff, J. P., Seth, N., Amirkhosravi, A., Amaya, M., Fogarty, S., Meyer, T. V., Siddiqui, F., and Francis, J. L. (1999) Soluble fibrin augments platelet/tumor cell adherence *in vitro* and *in vivo*, and enhances experimental metastasis. *Clin. Exp. Metastasis* **17,** 723–730
4. Ruf, W., and Edgington, T. S. (1994) Structural biology of tissue factor, the initiator of thrombogenesis *in vivo*. *FASEB J.* **8,** 385–390
5. Brummel, K. E., Paradis, S. G., Butenas, S., and Mann, K. G. (2002) Thrombin functions during tissue factor-induced blood coagulation. *Blood* **100,** 148–152
6. Mueller, B. M., Reisfeld, R. A., Edgington, T. S., and Ruf, W. (1992) Expression of tissue factor by melanoma cells promotes efficient hematogenous metastasis. *Proc. Natl. Acad. Sci. U.S.A.* **89,** 11832–11836
7. Hu, L., Lee, M., Campbell, W., Perez-Soler, R., and Karpatkin, S. (2004) Role of endogenous thrombin in tumor implantation, seeding, and spontaneous metastasis. *Blood* **104,** 2746–2751
8. Brose, M. S., Volpe, P., Feldman, M., Kumar, M., Rishi, I., Gerrero, R., Einhorn, E., Herlyn, M., Minna, J., Nicholson, A., Roth, J. A., Albelda, S. M., Davies, H., Cox, C., Brignell, G., *et al.* (2002) BRAF and RAS mutations in human lung cancer and melanoma. *Cancer Res.* **62,** 6997–7000
9. Davies, H., Bignell, G. R., Cox, C., Stephens, P., Edkins, S., Clegg, S., Teague, J., Woffendin, H., Garnett, M. J., Bottomley, W., Davis, N., Dicks, E., Ewing, R., Floyd, Y., Gray, K., *et al.* (2002) Mutations of the BRAF gene in human cancer. *Nature* **417,** 949–954
10. Millington, G. W. (2013) Mutations of the BRAF gene in human cancer, by Davies *et al.* (*Nature* 2002;417: 949–54). *Clin. Exp. Dermatol.* **38,** 222–223
11. Pollock, P. M., Harper, U. L., Hansen, K. S., Yudt, L. M., Stark, M., Robbins, C. M., Moses, T. Y., Hostetter, G., Wagner, U., Kakareka, J., Salem, G., Pohida, T., Heenan, P., Duray, P., Kallioniemi, O., *et al.* (2003) High frequency of BRAF mutations in nevi. *Nat. Genet.* **33,** 19–20
12. Mercer, K. E., and Pritchard, C. A. (2003) Raf proteins and cancer: B-Raf is identified as a mutational target. *Biochim. Biophys. Acta* **1653,** 25–40
13. Zhao, Y., Zhang, Y., Yang, Z., Li, A., and Dong, J. (2008) Simultaneous knockdown of BRAF and expression of INK4A in melanoma cells leads to potent growth inhibition and apoptosis. *Biochem. Biophys. Res. Commun.* **370,** 509–513
14. Lee, J. T., Li, L., Brafford, P. A., van den Eijnden, M., Halloran, M. B., Sproesser, K., Haass, N. K., Smalley, K. S., Tsai, J., Bollag, G., and Herlyn, M. (2010) PLX4032, a potent inhibitor of the B-Raf(V600E) oncogene, selectively inhibits V600E-positive melanomas. *Pigment Cell Melanoma Res* **23,** 820–827
15. Sharma, A., Tran, M. A., Liang, S., Sharma, A. K., Amin, S., Smith, C. D., Dong, C., and Robertson, G. P. (2006) Targeting mitogen-activated protein kinase/extracellular signal-regulated kinase kinase in the mutant (V600E) B-Raf signaling cascade effectively inhibits melanoma lung metastases. *Cancer Res.* **66,** 8200–8209
16. Liang, S., Sharma, A., Peng, H. H., Robertson, G., and Dong, C. (2007) Targeting mutant (V600E) B-Raf in melanoma interrupts immunoediting of leukocyte functions and melanoma extravasation. *Cancer Res.* **67,** 5814–5820
17. Rabiet, M. J., Plantier, J. L., Rival, Y., Genoux, Y., Lampugnani, M. G., and Dejana, E. (1996) Thrombin-induced increase in endothelial permeability is associated with changes in cell-to-cell junction organization. *Arterioscler. Thromb. Vasc. Biol.* **16,** 488–496
18. Konstantoulaki, M., Kouklis, P., and Malik, A. B. (2003) Protein kinase C modifications of VE-cadherin, p120, and β-catenin contribute to endothelial barrier dysregulation induced by thrombin. *Am. J. Physiol. Lung Cell. Mol. Physiol* **285,** L434–L442
19. Potter, M. D., Barbero, S., and Cheresh, D. A. (2005) Tyrosine phosphorylation of VE-cadherin prevents binding of p120- and β-catenin and maintains the cellular mesenchymal state. *J. Biol. Chem.* **280,** 31906–31912
20. Gavard, J., and Gutkind, J. S. (2006) VEGF controls endothelial-cell permeability by promoting the β-arrestin-dependent endocytosis of VE-cadherin. *Nat. Cell Biol.* **8,** 1223–1234
21. Dejana, E., Orsenigo, F., and Lampugnani, M. G. (2008) The role of adherens junctions and VE-cadherin in the control of vascular permeability. *J. Cell Sci.* **121,** 2115–2122
22. Peng, H. H., Liang, S., Henderson, A. J., and Dong, C. (2007) Regulation of interleukin-8 expression in melanoma-stimulated neutrophil inflammatory response. *Exp. Cell Res.* **313,** 551–559
23. Khanna, P., Yunkunis, T., Muddana, H. S., Peng, H. H., August, A., and Dong, C. (2010) p38 MAP kinase is necessary for melanoma-mediated regulation of VE-cadherin disassembly. *Am. J. Physiol. Cell Physiol* **298,** C1140–C1150
24. Orlova, V. V., Economopoulou, M., Lupu, F., Santoso, S., and Chavakis, T. (2006) Junctional adhesion molecule-C regulates vascular endothelial permeability by modulating VE-cadherin-mediated cell-cell contacts. *J. Exp. Med.* **203,** 2703–2714
25. Fukuhara, S., Sakurai, A., Sano, H., Yamagishi, A., Somekawa, S., Takakura, N., Saito, Y., Kangawa, K., and Mochizuki, N. (2005) Cyclic AMP potentiates vascular endothelial cadherin-mediated cell-cell contact to enhance endothelial barrier function through an Epac-Rap1 signaling pathway. *Mol. Cell. Biol.* **25,** 136–146
26. O'Hayer, K. M., and Counter, C. M. (2006) A genetically defined normal human somatic cell system to study ras oncogenesis *in vivo* and *in vitro*. *Methods Enzymol.* **407,** 637–647
27. Hodgson, L., Henderson, A. J., and Dong, C. (2003) Melanoma cell migration to type IV collagen requires activation of NF-κB. *Oncogene* **22,** 98–108
28. Slattery, M. J., Liang, S., and Dong, C. (2005) Distinct role of hydrodynamic shear in leukocyte-facilitated tumor cell extravasation. *Am. J. Physiol. Cell Physiol* **288,** C831–C839
29. Cheung, M., Sharma, A., Madhunapantula, S. V., and Robertson, G. P. (2008) Akt3 and mutant V600E B-Raf cooperate to promote early melanoma development. *Cancer Res.* **68,** 3429–3439
30. Bhatt, K. V., Spofford, L. S., Aram, G., McMullen, M., Pumiglia, K., and Aplin, A. E. (2005) Adhesion control of cyclin D1 and p27Kip1 levels is deregulated in melanoma cells through BRAF-MEK-ERK signaling. *Oncogene* **24,** 3459–3471
31. Joseph, E. W., Pratilas, C. A., Poulikakos, P. I., Tadi, M., Wang, W., Taylor, B. S., Halilovic, E., Persaud, Y., Xing, F., Viale, A., Tsai, J., Chapman, P. B., Bollag, G., Solit, D. B., and Rosen, N. (2010) The RAF inhibitor PLX4032 inhibits ERK signaling and tumor cell proliferation in a V600E BRAF-selective manner. *Proc. Natl. Acad. Sci. U.S.A.* **107,** 14903–14908
32. Sosman, J. A., Kim, K. B., Schuchter, L., Gonzalez, R., Pavlick, A. C., Weber, J. S., McArthur, G. A., Hutson, T. E., Moschos, S. J., Flaherty, K. T., Hersey, P., Kefford, R., Lawrence, D., Puzanov, I., Lewis, K. D., *et al.* (2012) Survival in BRAF V600-mutant advanced melanoma treated with vemurafenib. *N. Engl. J. Med.* **366,** 707–714
33. Huang, T., Zhuge, J., and Zhang, W. W. (2013) Sensitive detection of BRAF V600E mutation by Amplification Refractory Mutation System (ARMS)-PCR. *Biomark Res.* **1,** 3
34. Adam, A. P., Sharenko, A. L., Pumiglia, K., and Vincent, P. A. (2010) Src-induced tyrosine phosphorylation of VE-cadherin is not sufficient to

decrease barrier function of endothelial monolayers. *J. Biol. Chem.* **285,** 7045–7055
35. Gonzales, J. N., Kim, K. M., Zemskova, M. A., Rafikov, R., Heeke, B., Varn, M. N., Black, S., Kennedy, T. P., Verin, A. D., and Zemskov, E. A. (2014) Low anticoagulant heparin blocks thrombin-induced endothelial permeability in a PAR-dependent manner. *Vascul. Pharmacol.* **62,** 63–71
36. Sandoval, R., Malik, A. B., Minshall, R. D., Kouklis, P., Ellis, C. A., and Tiruppathi, C. (2001) $Ca^{2+}$ signalling and PKC$\alpha$ activate increased endothelial permeability by disassembly of VE-cadherin junctions. *J. Physiol.* **533,** 433–445
37. Liang, S., and Dong, C. (2008) Integrin VLA-4 enhances sialyl-Lewisx/a-negative melanoma adhesion to and extravasation through the endothelium under low flow conditions. *Am. J. Physiol. Cell Physiol* **295,** C701–C707
38. Zhang, P., Goodrich, C., Fu, C., and Dong, C. (2014) Melanoma upregulates ICAM-1 expression on endothelial cells through engagement of tumor CD44 with endothelial E-selectin and activation of a PKC$\alpha$-p38-SP-1 pathway. *FASEB J.* **28,** 4591–4609
39. Klein, R. M., Spofford, L. S., Abel, E. V., Ortiz, A., and Aplin, A. E. (2008) B-RAF regulation of Rnd3 participates in actin cytoskeletal and focal adhesion organization. *Mol. Biol. Cell* **19,** 498–508
40. Xiao, K., Garner, J., Buckley, K. M., Vincent, P. A., Chiasson, C. M., Dejana, E., Faundez, V., and Kowalczyk, A. P. (2005) p120-Catenin regulates clathrin-dependent endocytosis of VE-cadherin. *Mol. Biol. Cell* **16,** 5141–5151
41. Chiasson, C. M., Wittich, K. B., Vincent, P. A., Faundez, V., and Kowalczyk, A. P. (2009) p120-catenin inhibits VE-cadherin internalization through a Rho-independent mechanism. *Mol. Biol. Cell* **20,** 1970–1980
42. Hatanaka, K., Simons, M., and Murakami, M. (2011) Phosphorylation of VE-cadherin controls endothelial phenotypes via p120-catenin coupling and Rac1 activation. *Am. J. Physiol. Heart Circ. Physiol.* **300,** H162–H172
43. Xiao, K., Allison, D. F., Kottke, M. D., Summers, S., Sorescu, G. P., Faundez, V., and Kowalczyk, A. P. (2003) Mechanisms of VE-cadherin processing and degradation in microvascular endothelial cells. *J. Biol. Chem.* **278,** 19199–19208
44. Palacios, F., Tushir, J. S., Fujita, Y., and D'Souza-Schorey, C. (2005) Lysosomal targeting of E-cadherin: a unique mechanism for the down-regulation of cell-cell adhesion during epithelial to mesenchymal transitions. *Mol. Cell. Biol.* **25,** 389–402
45. Orsenigo, F., Giampietro, C., Ferrari, A., Corada, M., Galaup, A., Sigismund, S., Ristagno, G., Maddaluno, L., Koh, G. Y., Franco, D., Kurtcuoglu, V., Poulikakos, D., Baluk, P., McDonald, D., Grazia Lampugnani, M., and Dejana, E. (2012) Phosphorylation of VE-cadherin is modulated by haemodynamic forces and contributes to the regulation of vascular permeability *in vivo*. *Nat. Commun.* **3,** 1208
46. Rajput, C., Kini, V., Smith, M., Yazbeck, P., Chavez, A., Schmidt, T., Zhang, W., Knezevic, N., Komarova, Y., and Mehta, D. (2013) Neural Wiskott-Aldrich syndrome protein (N-WASP)-mediated p120-catenin interaction with Arp2-Actin complex stabilizes endothelial adherens junctions. *J. Biol. Chem.* **288,** 4241–4250
47. Vandenbroucke St Amant, E., Tauseef, M., Vogel, S. M., Gao, X. P., Mehta, D., Komarova, Y. A., and Malik, A. B. (2012) PKC$\alpha$ activation of p120-catenin serine 879 phospho-switch disassembles VE-cadherin junctions and disrupts vascular integrity. *Circ. Res.* **111,** 739–749
48. Yang, L., Froio, R. M., Sciuto, T. E., Dvorak, A. M., Alon, R., and Luscinskas, F. W. (2005) ICAM-1 regulates neutrophil adhesion and transcellular migration of TNF-$\alpha$-activated vascular endothelium under flow. *Blood* **106,** 584–592
49. Huh, S. J., Liang, S., Sharma, A., Dong, C., and Robertson, G. P. (2010) Transiently entrapped circulating tumor cells interact with neutrophils to facilitate lung metastasis development. *Cancer Res.* **70,** 6071–6082
50. Dong, C., Slattery, M. J., Liang, S., and Peng, H. H. (2005) Melanoma cell extravasation under flow conditions is modulated by leukocytes and endogenously produced interleukin 8. *Mol. Cell. Biomech.* **2,** 145–159
51. Whipple, C. A., and Brinckerhoff, C. E. (2014) BRAF(V600E) melanoma cells secrete factors that activate stromal fibroblasts and enhance tumourigenicity. *Br. J. Cancer* **111,** 1625–1633
52. Bhatt, K. V., Hu, R., Spofford, L. S., and Aplin, A. E. (2007) Mutant B-RAF signaling and cyclin D1 regulate Cks1/S-phase kinase-associated protein 2-mediated degradation of p27Kip1 in human melanoma cells. *Oncogene* **26,** 1056–1066
53. Xu, C., Gui, Q., Chen, W., Wu, L., Sun, W., Zhang, N., Xu, Q., Wang, J., and Fu, X. (2011) Small interference RNA targeting tissue factor inhibits human lung adenocarcinoma growth *in vitro* and *in vivo*. *J. Exp. Clin. Cancer Res.* **30,** 63
54. Yu, J. L., Xing, R., Milsom, C., and Rak, J. (2010) Modulation of the oncogene-dependent tissue factor expression by kinase suppressor of ras 1. *Thromb. Res.* **126,** e6–10
55. Schaffner, F., and Ruf, W. (2009) Tissue factor and PAR2 signaling in the tumor microenvironment. *Arterioscler. Thromb. Vasc. Biol.* **29,** 1999–2004
56. Schraufstatter, I. U., Chung, J., and Burger, M. (2001) IL-8 activates endothelial cell CXCR1 and CXCR2 through Rho and Rac signaling pathways. *Am. J. Physiol. Lung Cell. Mol. Physiol* **280,** L1094–L1103
57. Tremblay, P. L., Auger, F. A., and Huot, J. (2006) Regulation of transendothelial migration of colon cancer cells by E-selectin-mediated activation of p38 and ERK MAP kinases. *Oncogene* **25,** 6563–6573
58. Fu, C., Tong, C., Wang, M., Gao, Y., Zhang, Y., Lü, S., Liang, S., Dong, C., and Long, M. (2011) Determining $\beta$2-integrin and intercellular adhesion molecule 1 binding kinetics in tumor cell adhesion to leukocytes and endothelial cells by a gas-driven micropipette assay. *J. Biol. Chem.* **286,** 34777–34787
59. Dong, C., Slattery, M., and Liang, S. (2005) Micromechanics of tumor cell adhesion and migration under dynamic flow conditions. *Front. Biosci.* **10,** 379–384
60. Welsh, J. D., Colace, T. V., Muthard, R. W., Stalker, T. J., Brass, L. F., and Diamond, S. L. (2012) Platelet-targeting sensor reveals thrombin gradients within blood clots forming in microfluidic assays and in mouse. *J. Thromb. Haemost.* **10,** 2344–2353
61. Lee, A. M., Tormoen, G. W., Kanso, E., McCarty, O. J., and Newton, P. K. (2012) Modeling and simulation of procoagulant circulating tumor cells in flow. *Front. Oncol.* **2,** 108
62. Dejana, E., Tournier-Lasserve, E., and Weinstein, B. M. (2009) The control of vascular integrity by endothelial cell junctions: molecular basis and pathological implications. *Dev. Cell* **16,** 209–221
63. Allport, J. R., Muller, W. A., and Luscinskas, F. W. (2000) Monocytes induce reversible focal changes in vascular endothelial cadherin complex during transendothelial migration under flow. *J. Cell Biol.* **148,** 203–216
64. Shaw, S. K., Bamba, P. S., Perkins, B. N., and Luscinskas, F. W. (2001) Real-time imaging of vascular endothelial-cadherin during leukocyte transmigration across endothelium. *J. Immunol.* **167,** 2323–2330
65. Wessel, F., Winderlich, M., Holm, M., Frye, M., Rivera-Galdos, R., Vockel, M., Linnepe, R., Ipe, U., Stadtmann, A., Zarbock, A., Nottebaum, A. F., and Vestweber, D. (2014) Leukocyte extravasation and vascular permeability are each controlled *in vivo* by different tyrosine residues of VE-cadherin. *Nat. Immunol.* **15,** 223–230
66. Xiao, K., Allison, D. F., Buckley, K. M., Kottke, M. D., Vincent, P. A., Faundez, V., and Kowalczyk, A. P. (2003) Cellular levels of p120 catenin function as a set point for cadherin expression levels in microvascular endothelial cells. *J. Cell Biol.* **163,** 535–545
67. Vouret-Craviari, V., Boquet, P., Pouysségur, J., and Van Obberghen-Schilling, E. (1998) Regulation of the actin cytoskeleton by thrombin in human endothelial cells: role of Rho proteins in endothelial barrier function. *Mol. Biol. Cell* **9,** 2639–2653
68. Khuon, S., Liang, L., Dettman, R. W., Sporn, P. H., Wysolmerski, R. B., and Chew, T. L. (2010) Myosin light chain kinase mediates transcellular intravasation of breast cancer cells through the underlying endothelial cells: a three-dimensional FRET study. *J. Cell Sci.* **123,** 431–440
69. Gong, H., Gao, X., Feng, S., Siddiqui, M. R., Garcia, A., Bonini, M. G., Komarova, Y., Vogel, S. M., Mehta, D., and Malik, A. B. (2014) Evidence of a common mechanism of disassembly of adherens junctions through G$\alpha$13 targeting of VE-cadherin. *J. Exp. Med.* **211,** 579–591
70. Khanna, P., Chung, C. Y., Neves, R. I., Robertson, G. P., and Dong, C. (2014) CD82/KAI expression prevents IL-8-mediated endothelial gap formation in late-stage melanomas. *Oncogene* **33,** 2898–2908